

ON THE CHROMOSPHERIC ACTIVITY NATURE OF A LOW-MASS CLOSE BINARY: KIC 12004834

E. Yoldaş and H. A. Dal

Department of Astronomy and Space Sciences, University of Ege, Bornova, İzmir, Turkey.

Received June 10 2018; accepted January 17 2019

ABSTRACT

We study the nature of the chromospheric activity of an eclipsing binary KIC 12004834, using Kepler data. We analyse the light curve of the system, the sinusoidal variations at out-of-eclipses and detected flare events. The secondary component's temperature is found to be 4001 ± 11 K, the mass ratio is 0.743 ± 0.001 , and the orbital inclination is $75^\circ.89 \pm 0^\circ.03$. The analysis indicates a stellar spot effect on the variation. Moreover, the OPEA model has been derived over 149 flares. The saturation level called *Plateau* value, is found to be 2.093 ± 0.236 s. The flare number per hour (known as flare frequency N_1) is found to be $0.06644 h^{-1}$, while the flare-equivalent duration per hour (known as flare frequency N_2) is found to be 0.59 second/hour. According to these results, KIC 12004834 is a very low-mass close binary system with high level of flare activity.

RESUMEN

Estudiamos la actividad cromosférica de la binaria eclipsante KIC 12004834 utilizando datos de Kepler. Analizamos la curva de luz y la variación sinusoidal fuera de eclipse, y detectamos ráfagas. Encontramos que la temperatura de la secundaria es de 4001 ± 11 K, que el cociente de masas es 0.743 ± 0.001 y la inclinación orbital es $75^\circ.89 \pm 0^\circ.03$. El análisis indica que hay un efecto de manchas en la variabilidad. Obtenemos el modelo OPEA para 149 ráfagas. El nivel de saturación, llamado *Plateau* tiene un valor de 2.093 ± 0.236 s. El número de ráfagas por hora, conocido como la frecuencia de ráfagas N_1 , es $0.06644 h^{-1}$, mientras que la duración de la emisión equivalente a las ráfagas, conocida como la frecuencia N_2 es 0.59 s/hora. De acuerdo con estos resultados, KIC 12004834 es una binaria cerrada, de muy baja masa, y con frecuentes ráfagas.

Key Words: binaries: eclipsing — methods: data analysis — stars: flare — stars: individual: KIC 12004834 — stars: low-mass — techniques: photometric

1. INTRODUCTION

The nature of a low-mass eclipsing binary KIC 12004834 with $14^m.7180$ in Kepler band is studied here. KIC 12004834, whose nature is different from the classical UV Ceti type stars of spectral type dMe due to its being a binary system, was observed by Watson (2006) for the first time. Magnitudes of the system were given as $J = 12^m.007$, $H = 11^m.407$, $K = 11^m.170$ by Cutri et al. (2003). Although there are no further studies in the literature, some estimated parameters of the system were

given by Coughlin et al. (2011), using calibrations to derive the parameters. Taking $T_{\text{eff}} = 3576$ K, the orbital inclination (i) was found to be $72^\circ.47$, while the masses were found to be $M_1 = 0.48 M_\odot$ and $M_2 = 0.34 M_\odot$. In addition, the radii were computed as $R_1 = 0.48 R_\odot$ and $R_2 = 0.35 R_\odot$. Like Coughlin et al. (2011), taking $T_{\text{eff}} = 3576$ K, Slawson et al. (2011) found $\log(g)$ as 4.217 cm/s^2 . There are several approaches to obtain the temperatures of its components. Coughlin et al. (2011) gave the temperatures as $T_1 = 3620$ K for the pri-

mary and $T_2 = 3468$ K for the secondary. Armstrong et al. (2014) gave $T_1 = 3511$ K for the primary and $T_2 = 3512$ K for the secondary.

KIC 12004834 was mentioned as a chromospherically active system for the first time by Debosscher et al. (2011). In addition, a dominant flare activity was also reported by Balona (2015). Considering the estimated parameters of the system; KIC 12004834 is a low-mass close binary with a chromospherically active component. This makes the system an important object in the astrophysical sense. This is because the system exhibits not only spots, but also flare activity. A flaring star being a component of an eclipsing binary system is a rare phenomenon among the UV Ceti type stars. However, the red dwarf abundance is about 65% in our Galaxy, and seventy-five percent of them exhibit flare activity (Rodonó 1986). Thus, almost half of the stars in our galaxy should exhibit flare activity. The number of eclipsing binaries with a flaring component is nowadays increasing, thanks to space missions such the Kepler and Corot satellites.

Because of its effects on stellar evolution, flare activity is very important in astrophysics in terms of its sources and mechanism. Although the first flare was observed on the solar surface by R. C. Carrington and R. Hodgson on September 1, 1859 (Carrington 1859; Hodgson 1859), there are still unsolved problems, for instance, the different mass loss rate seen among stars of different spectral types, the different flare energy levels detected for stars of different spectral types (Gershberg & Shakhovskaya 1983; Haisch et al. 1991; Gershberg 2005; Benz 2008).

At this point, photometric data accumulated from the eclipsing binaries with a chromospherically active component can give some clues for these problems. Recently, several eclipsing binary stars, where one of the components is chromospherically active have been discovered by the Kepler Mission (Borucki et al. 2010; Koch et al. 2010; Caldwell et al. 2010). Most of them have an interesting nature. These chromospherically active components exhibit flare events and also rapidly evolving stellar spots (Balona 2015). Although the light variations due to the cool spots have remarkably small amplitudes, their shapes change over short time intervals, from one cycle to the next one (Yoldas & Dal 2016, 2017; Özdarcan et al. 2017).

In this study, the variations of the times of minima are analysed (see § 2.1). The light curve of KIC 12004834 is studied (§ 2.2) for the first time in the literature in order to find the physical properties of the components. Then, the flares occurring

on the chromospherically active component are used to model the nature of the magnetic activity of the system as described in § 2.3. The results obtained are given in § 3, comparing the active component with its analogue discovered in the Kepler Mission.

2. DATA AND ANALYSES

The data analysed in this study are the detrended short cadence data from the Kepler Mission Database (Borucki et al. 2010; Koch et al. 2010; Caldwell et al. 2010; Slawson et al. 2011; Matijević et al. 2012). In the analyses, the data of quarters Q10.1, Q10.2 and Q10.3 are used (Murphy 2012; Murphy et al. 2013), whose quality and sensitivity are the highest ones ever reached (Jenkins et al. 2010a,b).

After removing all the observations with large errors from the data, and using the ephemeris taken from the Kepler Mission database, the phases are computed for all data, and the obtained light curves are shown in Figure 1. Because of the study's format, the detrended short cadence data were used in the analysis instead of those of the long cadence. The data were arranged in suitable formats for different analyses, such as the light curve analysis and the flare event calculations.

2.1. Orbital Period Variation

The times of minima in the light curves were computed from short cadence data without any corrections. We used just short cadence data, because the system has a very short orbital period. The whole shape of the minima is not seen in the long cadence data. The minima times were computed with a script according to the method described by Kwee & van Woerden (1956). The $(O - C)_I$ residuals were determined for each minimum time. Examining the times of minima indicated that some of them have very large errors. These errors are sometimes caused by scattered observations; while some of them are caused by the flare activity occurring during these minima. All the minima times with large errors were removed from the $(O - C)$ data. Finally, 688 minima times were determined in the analyses.

Using the epoch of 2455002.041 and the orbital period of 0.2623168 day given in the Kepler Eclipsing Binary Catalogue¹ by Slawson et al. (2011), we computed the $(O - C)_I$ residuals. Then, using the Least-Squares method, we applied a linear correction to these residuals. The linear correction revealed that the $(O - C)_I$ residuals had a linear trend with

¹<http://keplerebs.villanova.edu/>.

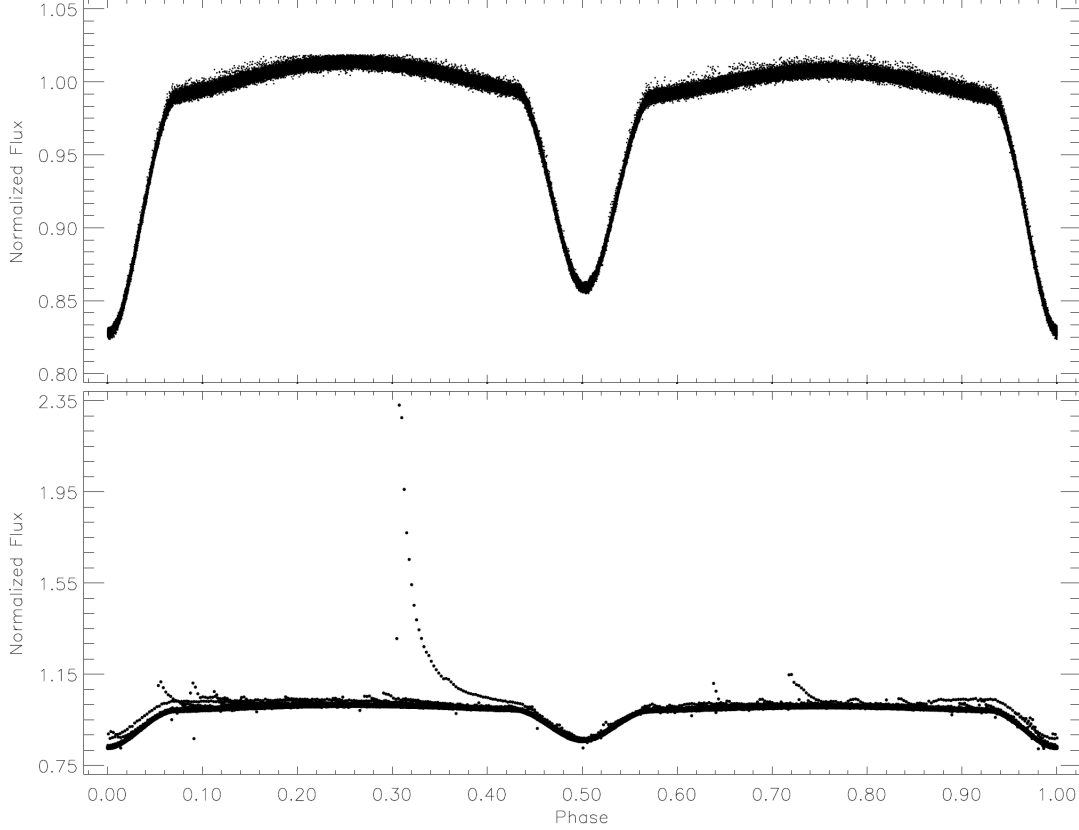


Fig. 1. Whole light curve of KIC 12004834 obtained from the data taken from the Kepler Mission database. In the bottom panel, the light curve is plotted along the orbital cycle with the flare activity, while it is plotted without the flare activity in the upper panel.

a small slope; the distribution of the $(O - C)_I$ residuals seems to be linear, needing just a zero point correction. After the linear correction, we obtained the new ephemerides given in equation (1) and the $(O - C)_{II}$ residuals:

$$JD(Bary.) = 24\ 55002.04164(14) + 0^d.262317(1) \times E. \quad (1)$$

The $(O - C)_I$ and $(O - C)_{II}$ residuals are listed in Table 1. In the table, the minima times, cycles, the minima type, $(O - C)_I$ and $(O - C)_{II}$ residuals are listed, respectively. An interesting variation is seen in the $(O - C)_{II}$ residuals plotted versus time in Figure 2.

According to the studies of Tran et al. (2013) on contact binaries, if one of the components of an eclipsing binary system exhibits stellar spot activity on its surface, there must be a separation between the $(O - C)_{II}$ residuals of the primary and secondary minima. Debosscher et al. (2011) and Balona (2015) mentioned that the system exhibits chromospheric

activity. In the case of KIC 12004834 considered as a very close binary, we firstly examined whether there was any separation in the primary and secondary minimum $(O - C)_{II}$ residuals. As shown in the upper panel of Figure 2, there is an evident separation between the primary and secondary minima residuals. Secondly, the analysis indicates that the best fit is derived by a linear function for the distribution of $(O - C)_I$. The obtained fit is shown in the lower panel of is Figure 2.

2.2. Light Curve Analysis

The light curve of KIC 12004834 was analyzed by the PHOEBE V.0.32 software (Prša & Zwitter 2005) which depends on the 2003 version of the Wilson-Devinney Code (Wilson & Devinney 1971; Wilson 1990) to compute the physical parameters of each component. In the analyses, the averaged data were computed phase by phase with an interval of 0.001 to decrease the scattering. Although several modes

TABLE 1
MINIMA TIMES AND THEIR RESIDUALS

BJD (+24 50000)	E	Type	$(O - C)_I$ (day)	$(O - C)_{II}$ (day)	BJD (+24 50000)	E	Type	$(O - C)_I$ (day)	$(O - C)_{II}$ (day)
5739.93853	2813.0	I	0.00037	-0.00014	5833.06104	3168.0	I	0.00041	-0.00008
5740.20090	2814.0	I	0.00042	-0.00009	5740.06987	2813.5	II	0.00055	0.00004
5740.46318	2815.0	I	0.00039	-0.00013	5740.33222	2814.5	II	0.00059	0.00007
5740.72552	2816.0	I	0.00041	-0.00010	5740.59460	2815.5	II	0.00065	0.00013
5740.98782	2817.0	I	0.00040	-0.00012	5740.85687	2816.5	II	0.00060	0.00008
5741.25018	2818.0	I	0.00044	-0.00008	5741.11948	2817.5	II	0.00090	0.00038
5741.51253	2819.0	I	0.00047	-0.00004	5741.38143	2818.5	II	0.00053	0.00001
5741.77485	2820.0	I	0.00047	-0.00004	5741.64370	2819.5	II	0.00049	-0.00003
5742.03709	2821.0	I	0.00040	-0.00011	5741.90610	2820.5	II	0.00056	0.00005
5742.29950	2822.0	I	0.00049	-0.00002	5742.16839	2821.5	II	0.00054	0.00003
5742.56182	2823.0	I	0.00049	-0.00002	5742.43077	2822.5	II	0.00060	0.00008
5742.82406	2824.0	I	0.00042	-0.00009	5742.69298	2823.5	II	0.00049	-0.00002
5743.08650	2825.0	I	0.00054	0.00003	5742.95537	2824.5	II	0.00057	0.00006
5743.34869	2826.0	I	0.00041	-0.00010	5743.21765	2825.5	II	0.00053	0.00002
5743.61107	2827.0	I	0.00048	-0.00003	5743.47996	2826.5	II	0.00052	0.00001
5743.87339	2828.0	I	0.00048	-0.00003	5743.74229	2827.5	II	0.00054	0.00003
5744.13561	2829.0	I	0.00038	-0.00013	5744.00469	2828.5	II	0.00062	0.00011
5744.39801	2830.0	I	0.00046	-0.00005	5744.26691	2829.5	II	0.00052	0.00001
5744.66025	2831.0	I	0.00038	-0.00013	5744.52938	2830.5	II	0.00068	0.00016
5744.92283	2832.0	I	0.00065	0.00014	5744.79153	2831.5	II	0.00051	0.00000
5745.18490	2833.0	I	0.00041	-0.00010	5745.05391	2832.5	II	0.00058	0.00006
5745.44729	2834.0	I	0.00048	-0.00003	5745.31632	2833.5	II	0.00067	0.00015
5745.70963	2835.0	I	0.00050	-0.00001	5745.57862	2834.5	II	0.00065	0.00013
5745.97188	2836.0	I	0.00044	-0.00007	5745.84093	2835.5	II	0.00064	0.00013
5746.23418	2837.0	I	0.00041	-0.00010	5746.10319	2836.5	II	0.00059	0.00008
5746.49653	2838.0	I	0.00046	-0.00006	5746.36550	2837.5	II	0.00058	0.00007
5746.75883	2839.0	I	0.00044	-0.00007	5746.62782	2838.5	II	0.00058	0.00007
5747.02101	2840.0	I	0.00030	-0.00021	5746.89012	2839.5	II	0.00057	0.00006
5747.28347	2841.0	I	0.00044	-0.00007	5747.15246	2840.5	II	0.00059	0.00008
5747.54575	2842.0	I	0.00040	-0.00011	5747.41478	2841.5	II	0.00060	0.00008
5747.80808	2843.0	I	0.00042	-0.00009	5747.67710	2842.5	II	0.00059	0.00008
5748.07045	2844.0	I	0.00047	-0.00005	5747.93950	2843.5	II	0.00068	0.00017
5748.33278	2845.0	I	0.00048	-0.00003	5748.20170	2844.5	II	0.00056	0.00005
5748.59497	2846.0	I	0.00035	-0.00016	5748.46406	2845.5	II	0.00061	0.00009
5748.85738	2847.0	I	0.00045	-0.00006	5748.72647	2846.5	II	0.00069	0.00018
5749.11974	2848.0	I	0.00049	-0.00002	5748.98876	2847.5	II	0.00067	0.00016
5749.38192	2849.0	I	0.00036	-0.00016	5749.25105	2848.5	II	0.00065	0.00013
5749.64431	2850.0	I	0.00043	-0.00008	5749.51321	2849.5	II	0.00049	-0.00002
5749.90661	2851.0	I	0.00042	-0.00009	5749.77566	2850.5	II	0.00062	0.00011
5750.16895	2852.0	I	0.00043	-0.00008	5750.03785	2851.5	II	0.00050	-0.00002
5750.43123	2853.0	I	0.00040	-0.00011	5750.30019	2852.5	II	0.00052	0.00001
5750.69361	2854.0	I	0.00046	-0.00005	5750.56269	2853.5	II	0.00070	0.00019
5750.95592	2855.0	I	0.00046	-0.00005	5750.82496	2854.5	II	0.00066	0.00014
5751.21813	2856.0	I	0.00035	-0.00016	5751.08720	2855.5	II	0.00058	0.00007
5751.48043	2857.0	I	0.00033	-0.00018	5751.34962	2856.5	II	0.00068	0.00017
5751.74287	2858.0	I	0.00045	-0.00006	5751.61171	2857.5	II	0.00046	-0.00005
5752.00513	2859.0	I	0.00039	-0.00012	5751.87418	2858.5	II	0.00060	0.00009
5752.26744	2860.0	I	0.00039	-0.00012	5752.13672	2859.5	II	0.00083	0.00032
5752.52964	2861.0	I	0.00027	-0.00024	5752.39881	2860.5	II	0.00060	0.00009
5752.79203	2862.0	I	0.00034	-0.00017	5752.66107	2861.5	II	0.00055	0.00004
5753.05428	2863.0	I	0.00028	-0.00023	5752.92340	2862.5	II	0.00056	0.00005
5753.31685	2864.0	I	0.00054	0.00003	5753.18572	2863.5	II	0.00056	0.00005

TABLE 1 (CONTINUED)

BJD (+24 50000)	E	Type	$(O - C)_I$ (day)	$(O - C)_{II}$ (day)	BJD (+24 50000)	E	Type	$(O - C)_I$ (day)	$(O - C)_{II}$ (day)
5753.57902	2865.0	I	0.00039	-0.00012	5753.44802	2864.5	II	0.00054	0.00003
5753.84128	2866.0	I	0.00033	-0.00018	5753.71046	2865.5	II	0.00067	0.00016
5754.10358	2867.0	I	0.00031	-0.00020	5753.97273	2866.5	II	0.00063	0.00012
5754.36600	2868.0	I	0.00042	-0.00009	5754.23500	2867.5	II	0.00058	0.00007
5754.62820	2869.0	I	0.00030	-0.00021	5754.49742	2868.5	II	0.00068	0.00017
5754.89082	2870.0	I	0.00060	0.00009	5754.75969	2869.5	II	0.00063	0.00012
5755.15292	2871.0	I	0.00039	-0.00012	5755.02200	2870.5	II	0.00062	0.00011
5755.41537	2872.0	I	0.00053	0.00001	5755.28431	2871.5	II	0.00062	0.00011
5755.67762	2873.0	I	0.00045	-0.00006	5755.54643	2872.5	II	0.00042	-0.00009
5755.93995	2874.0	I	0.00047	-0.00004	5755.80900	2873.5	II	0.00068	0.00017
5756.20219	2875.0	I	0.00039	-0.00013	5756.07126	2874.5	II	0.00062	0.00011
5756.46450	2876.0	I	0.00038	-0.00013	5756.33364	2875.5	II	0.00068	0.00017
5756.72679	2877.0	I	0.00036	-0.00015	5756.59594	2876.5	II	0.00066	0.00015
5757.25137	2879.0	I	0.00030	-0.00021	5756.85817	2877.5	II	0.00058	0.00007
5757.51358	2880.0	I	0.00019	-0.00032	5757.12057	2878.5	II	0.00066	0.00015
5757.77606	2881.0	I	0.00036	-0.00015	5757.38280	2879.5	II	0.00058	0.00007
5758.03841	2882.0	I	0.00039	-0.00012	5757.64519	2880.5	II	0.00065	0.00014
5758.30065	2883.0	I	0.00032	-0.00019	5757.90742	2881.5	II	0.00056	0.00005
5758.56303	2884.0	I	0.00037	-0.00014	5758.16977	2882.5	II	0.00060	0.00009
5758.82529	2885.0	I	0.00032	-0.00019	5758.43218	2883.5	II	0.00069	0.00018
5759.08774	2886.0	I	0.00045	-0.00006	5758.69452	2884.5	II	0.00071	0.00020
5759.35011	2887.0	I	0.00051	-0.00001	5758.95684	2885.5	II	0.00072	0.00021
5759.61229	2888.0	I	0.00037	-0.00014	5759.21913	2886.5	II	0.00068	0.00017
5759.87448	2889.0	I	0.00025	-0.00026	5759.48141	2887.5	II	0.00065	0.00014
5760.13695	2890.0	I	0.00039	-0.00012	5759.74364	2888.5	II	0.00056	0.00005
5760.39929	2891.0	I	0.00042	-0.00009	5760.06063	2889.5	II	0.00063	0.00012
5760.66157	2892.0	I	0.00038	-0.00013	5760.26829	2890.5	II	0.00058	0.00007
5760.92396	2893.0	I	0.00046	-0.00005	5760.53054	2891.5	II	0.00052	0.00001
5761.18628	2894.0	I	0.00046	-0.00005	5760.79294	2892.5	II	0.00059	0.00008
5761.44852	2895.0	I	0.00039	-0.00012	5761.05529	2893.5	II	0.00063	0.00012
5761.71085	2896.0	I	0.00040	-0.00011	5761.31752	2894.5	II	0.00054	0.00003
5761.97323	2897.0	I	0.00046	-0.00005	5761.57990	2895.5	II	0.00061	0.00010
5762.23551	2898.0	I	0.00042	-0.00009	5761.84227	2896.5	II	0.00066	0.00015
5762.49784	2899.0	I	0.00043	-0.00008	5762.10455	2897.5	II	0.00062	0.00011
5762.76015	2900.0	I	0.00043	-0.00008	5762.36681	2898.5	II	0.00056	0.00005
5763.02252	2901.0	I	0.00048	-0.00003	5762.62918	2899.5	II	0.00062	0.00011
5763.28483	2902.0	I	0.00047	-0.00004	5762.89124	2900.5	II	0.00037	-0.00014
5763.54712	2903.0	I	0.00045	-0.00006	5763.15403	2901.5	II	0.00083	0.00032
5763.80947	2904.0	I	0.00048	-0.00003	5763.41597	2902.5	II	0.00046	-0.00005
5764.07172	2905.0	I	0.00041	-0.00010	5763.67842	2903.5	II	0.00059	0.00008
5764.33411	2906.0	I	0.00049	-0.00002	5763.94075	2904.5	II	0.00061	0.00010
5764.59645	2907.0	I	0.00051	0.00000	5764.20278	2905.5	II	0.00032	-0.00019
5764.85872	2908.0	I	0.00047	-0.00004	5764.46537	2906.5	II	0.00059	0.00008
5765.12109	2909.0	I	0.00052	0.00001	5764.72771	2907.5	II	0.00062	0.00011
5765.38338	2910.0	I	0.00049	-0.00002	5764.99002	2908.5	II	0.00061	0.00010
5765.64561	2911.0	I	0.00040	-0.00011	5765.25234	2909.5	II	0.00061	0.00010
5765.90796	2912.0	I	0.00044	-0.00007	5765.51464	2910.5	II	0.00059	0.00008
5766.17027	2913.0	I	0.00043	-0.00008	5765.77706	2911.5	II	0.00070	0.00019
5766.43259	2914.0	I	0.00043	-0.00008	5766.03932	2912.5	II	0.00064	0.00013
5766.69492	2915.0	I	0.00045	-0.00006	5766.30149	2913.5	II	0.00049	-0.00002
5766.95725	2916.0	I	0.00046	-0.00005	5766.56391	2914.5	II	0.00059	0.00008
5767.21957	2917.0	I	0.00046	-0.00004	5766.82620	2915.5	II	0.00057	0.00006
5767.48203	2918.0	I	0.00060	0.00010	5767.08856	2916.5	II	0.00061	0.00010
5767.74426	2919.0	I	0.00053	0.00002	5767.35084	2917.5	II	0.00057	0.00006

TABLE 1 (CONTINUED)

BJD (+24 50000)	E	Type	$(O - C)_I$ (day)	$(O - C)_{II}$ (day)	BJD (+24 50000)	E	Type	$(O - C)_I$ (day)	$(O - C)_{II}$ (day)
5768.00651	2920.0	I	0.00045	-0.00006	5767.61314	2918.5	II	0.00056	0.00005
5768.26882	2921.0	I	0.00044	-0.00006	5767.87550	2919.5	II	0.00060	0.00009
5768.53113	2922.0	I	0.00044	-0.00006	5768.13771	2920.5	II	0.00049	-0.00001
5768.79353	2923.0	I	0.00052	0.00002	5768.40024	2921.5	II	0.00071	0.00020
5769.05572	2924.0	I	0.00040	-0.00011	5768.66241	2922.5	II	0.00056	0.00006
5769.31808	2925.0	I	0.00044	-0.00007	5768.92476	2923.5	II	0.00059	0.00009
5769.58036	2926.0	I	0.00041	-0.00010	5769.18702	2924.5	II	0.00053	0.00003
5769.84269	2927.0	I	0.00042	-0.00009	5769.44938	2925.5	II	0.00058	0.00007
5770.89201	2931.0	I	0.00047	-0.00004	5769.71170	2926.5	II	0.00058	0.00007
5771.15430	2932.0	I	0.00044	-0.00007	5771.02329	2931.5	II	0.00059	0.00009
5771.41653	2933.0	I	0.00035	-0.00015	5771.28561	2932.5	II	0.00059	0.00008
5771.67891	2934.0	I	0.00042	-0.00009	5771.54806	2933.5	II	0.00073	0.00022
5771.94126	2935.0	I	0.00045	-0.00006	5771.81024	2934.5	II	0.00059	0.00008
5772.20359	2936.0	I	0.00047	-0.00004	5772.07252	2935.5	II	0.00055	0.00004
5772.46592	2937.0	I	0.00048	-0.00003	5772.33480	2936.5	II	0.00052	0.00001
5772.72823	2938.0	I	0.00047	-0.00003	5772.59722	2937.5	II	0.00062	0.00011
5772.99053	2939.0	I	0.00046	-0.00005	5772.85951	2938.5	II	0.00060	0.00009
5773.25281	2940.0	I	0.00041	-0.00009	5773.12172	2939.5	II	0.00048	-0.00002
5773.77750	2942.0	I	0.00047	-0.00004	5773.38416	2940.5	II	0.00061	0.00011
5774.03976	2943.0	I	0.00042	-0.00009	5773.64643	2941.5	II	0.00057	0.00006
5774.30213	2944.0	I	0.00047	-0.00004	5773.90875	2942.5	II	0.00056	0.00005
5774.56442	2945.0	I	0.00044	-0.00007	5774.17113	2943.5	II	0.00063	0.00012
5774.82673	2946.0	I	0.00044	-0.00007	5774.43336	2944.5	II	0.00055	0.00004
5775.08902	2947.0	I	0.00041	-0.00010	5774.69576	2945.5	II	0.00063	0.00012
5775.35138	2948.0	I	0.00045	-0.00006	5774.95804	2946.5	II	0.00059	0.00008
5775.61364	2949.0	I	0.00040	-0.00011	5775.22027	2947.5	II	0.00051	0.00000
5775.87595	2950.0	I	0.00039	-0.00011	5775.48274	2948.5	II	0.00065	0.00014
5776.13830	2951.0	I	0.00042	-0.00009	5775.74500	2949.5	II	0.00060	0.00009
5776.40067	2952.0	I	0.00047	-0.00004	5776.00734	2950.5	II	0.00062	0.00011
5776.66298	2953.0	I	0.00047	-0.00003	5776.26960	2951.5	II	0.00057	0.00006
5776.92523	2954.0	I	0.00041	-0.00010	5776.53194	2952.5	II	0.00059	0.00008
5777.18759	2955.0	I	0.00044	-0.00006	5776.79429	2953.5	II	0.00062	0.00011
5777.44985	2956.0	I	0.00039	-0.00011	5777.05653	2954.5	II	0.00055	0.00004
5777.71216	2957.0	I	0.00038	-0.00013	5777.31886	2955.5	II	0.00056	0.00005
5777.97445	2958.0	I	0.00036	-0.00015	5777.58118	2956.5	II	0.00056	0.00005
5778.23677	2959.0	I	0.00036	-0.00015	5777.84361	2957.5	II	0.00067	0.00017
5778.49912	2960.0	I	0.00039	-0.00011	5778.10584	2958.5	II	0.00059	0.00008
5778.76147	2961.0	I	0.00042	-0.00008	5778.36816	2959.5	II	0.00059	0.00008
5779.02378	2962.0	I	0.00042	-0.00009	5778.63048	2960.5	II	0.00060	0.00009
5779.28609	2963.0	I	0.00041	-0.00009	5778.89269	2961.5	II	0.00049	-0.00002
5779.54846	2964.0	I	0.00047	-0.00004	5779.15504	2962.5	II	0.00052	0.00001
5779.81070	2965.0	I	0.00039	-0.00012	5779.41739	2963.5	II	0.00056	0.00005
5780.07298	2966.0	I	0.00035	-0.00015	5779.67979	2964.5	II	0.00063	0.00013
5780.33536	2967.0	I	0.00042	-0.00009	5779.94215	2965.5	II	0.00068	0.00017
5780.59768	2968.0	I	0.00042	-0.00009	5780.20452	2966.5	II	0.00073	0.00022
5780.85996	2969.0	I	0.00038	-0.00012	5780.46661	2967.5	II	0.00051	0.00000
5781.12228	2970.0	I	0.00039	-0.00012	5780.72892	2968.5	II	0.00050	-0.00001
5781.38458	2971.0	I	0.00037	-0.00014	5780.99127	2969.5	II	0.00053	0.00003
5781.64690	2972.0	I	0.00037	-0.00014	5781.25359	2970.5	II	0.00053	0.00003
5781.90926	2973.0	I	0.00042	-0.00009	5781.51601	2971.5	II	0.00063	0.00013
5782.17159	2974.0	I	0.00042	-0.00008	5781.77844	2972.5	II	0.00075	0.00025
5782.43385	2975.0	I	0.00037	-0.00014	5782.04071	2973.5	II	0.00071	0.00020
5782.69628	2976.0	I	0.00049	-0.00002	5782.30292	2974.5	II	0.00059	0.00009
5782.95845	2977.0	I	0.00033	-0.00017	5782.56533	2975.5	II	0.00070	0.00019

TABLE 1 (CONTINUED)

BJD (+24 50000)	E	Type	$(O - C)_I$ (day)	$(O - C)_{II}$ (day)	BJD (+24 50000)	E	Type	$(O - C)_I$ (day)	$(O - C)_{II}$ (day)
5783.22076	2978.0	I	0.00033	-0.00017	5782.82763	2976.5	II	0.00067	0.00017
5783.48316	2979.0	I	0.00042	-0.00009	5783.08978	2977.5	II	0.00051	0.00000
5783.74559	2980.0	I	0.00052	0.00002	5783.35222	2978.5	II	0.00063	0.00013
5784.00765	2981.0	I	0.00027	-0.00023	5783.61454	2979.5	II	0.00064	0.00013
5784.27018	2982.0	I	0.00049	-0.00002	5783.87685	2980.5	II	0.00063	0.00012
5784.53237	2983.0	I	0.00036	-0.00015	5784.13909	2981.5	II	0.00055	0.00004
5784.79470	2984.0	I	0.00037	-0.00014	5784.40146	2982.5	II	0.00061	0.00010
5785.05708	2985.0	I	0.00043	-0.00007	5784.66373	2983.5	II	0.00056	0.00005
5785.31938	2986.0	I	0.00041	-0.00009	5784.92628	2984.5	II	0.00079	0.00029
5785.58162	2987.0	I	0.00033	-0.00017	5785.18850	2985.5	II	0.00070	0.00019
5785.84400	2988.0	I	0.00040	-0.00011	5785.45072	2986.5	II	0.00060	0.00010
5786.10633	2989.0	I	0.00041	-0.00009	5785.71294	2987.5	II	0.00050	0.00000
5786.36872	2990.0	I	0.00049	-0.00002	5786.23768	2989.5	II	0.00060	0.00010
5786.63076	2991.0	I	0.00021	-0.00029	5786.49999	2990.5	II	0.00060	0.00009
5786.89323	2992.0	I	0.00036	-0.00014	5786.76227	2991.5	II	0.00057	0.00006
5787.15562	2993.0	I	0.00044	-0.00007	5787.02466	2992.5	II	0.00064	0.00013
5787.41789	2994.0	I	0.00039	-0.00012	5787.28710	2993.5	II	0.00076	0.00025
5787.68022	2995.0	I	0.00040	-0.00011	5787.54920	2994.5	II	0.00054	0.00003
5787.94251	2996.0	I	0.00038	-0.00013	5787.81157	2995.5	II	0.00060	0.00009
5788.20475	2997.0	I	0.00030	-0.00020	5788.07397	2996.5	II	0.00068	0.00018
5788.46720	2998.0	I	0.00043	-0.00007	5788.33633	2997.5	II	0.00072	0.00021
5788.72942	2999.0	I	0.00034	-0.00017	5788.59842	2998.5	II	0.00050	-0.00001
5788.99177	3000.0	I	0.00037	-0.00014	5788.86078	2999.5	II	0.00053	0.00003
5789.25408	3001.0	I	0.00036	-0.00014	5789.12328	3000.5	II	0.00072	0.00022
5789.51641	3002.0	I	0.00038	-0.00013	5789.38556	3001.5	II	0.00069	0.00018
5789.77866	3003.0	I	0.00031	-0.00020	5789.64780	3002.5	II	0.00061	0.00010
5790.04109	3004.0	I	0.00042	-0.00008	5789.91000	3003.5	II	0.00050	-0.00001
5790.30352	3005.0	I	0.00053	0.00003	5790.17263	3004.5	II	0.00080	0.00030
5790.56574	3006.0	I	0.00044	-0.00007	5790.43473	3005.5	II	0.00058	0.00008
5790.82787	3007.0	I	0.00025	-0.00025	5790.69702	3006.5	II	0.00056	0.00006
5791.09036	3008.0	I	0.00042	-0.00008	5790.95941	3007.5	II	0.00064	0.00013
5791.35262	3009.0	I	0.00037	-0.00014	5791.22160	3008.5	II	0.00051	0.00000
5791.61493	3010.0	I	0.00037	-0.00014	5791.48409	3009.5	II	0.00068	0.00017
5791.87739	3011.0	I	0.00050	0.00000	5791.74635	3010.5	II	0.00062	0.00012
5792.13963	3012.0	I	0.00043	-0.00008	5792.00872	3011.5	II	0.00068	0.00017
5792.40196	3013.0	I	0.00044	-0.00007	5792.27091	3012.5	II	0.00055	0.00005
5792.66439	3014.0	I	0.00056	0.00005	5792.53334	3013.5	II	0.00066	0.00015
5792.92667	3015.0	I	0.00052	0.00002	5792.79570	3014.5	II	0.00071	0.00020
5793.18883	3016.0	I	0.00036	-0.00014	5793.05791	3015.5	II	0.00059	0.00009
5793.45125	3017.0	I	0.00046	-0.00004	5793.32014	3016.5	II	0.00051	0.00001
5793.71356	3018.0	I	0.00045	-0.00005	5793.58251	3017.5	II	0.00057	0.00007
5793.97583	3019.0	I	0.00042	-0.00009	5793.84439	3018.5	II	0.00013	-0.00038
5794.23824	3020.0	I	0.00050	0.00000	5794.10726	3019.5	II	0.00068	0.00018
5794.50047	3021.0	I	0.00042	-0.00009	5794.36953	3020.5	II	0.00063	0.00013
5795.02511	3023.0	I	0.00042	-0.00008	5794.63184	3021.5	II	0.00063	0.00012
5795.28743	3024.0	I	0.00042	-0.00008	5794.89418	3022.5	II	0.00065	0.00015
5795.54970	3025.0	I	0.00038	-0.00012	5795.15639	3023.5	II	0.00055	0.00004
5795.81201	3026.0	I	0.00037	-0.00013	5795.41861	3024.5	II	0.00045	-0.00006
5796.07435	3027.0	I	0.00040	-0.00011	5795.68117	3025.5	II	0.00069	0.00019
5796.33660	3028.0	I	0.00033	-0.00017	5795.94344	3026.5	II	0.00064	0.00014
5796.59882	3029.0	I	0.00023	-0.00027	5796.20583	3027.5	II	0.00072	0.00022
5796.86132	3030.0	I	0.00042	-0.00008	5796.46806	3028.5	II	0.00063	0.00013
5797.12378	3031.0	I	0.00056	0.00006	5796.73036	3029.5	II	0.00062	0.00011
5797.38596	3032.0	I	0.00042	-0.00008	5796.99260	3030.5	II	0.00054	0.00003

TABLE 1 (CONTINUED)

BJD (+24 50000)	E	Type	$(O - C)_I$ (day)	$(O - C)_{II}$ (day)	BJD (+24 50000)	E	Type	$(O - C)_I$ (day)	$(O - C)_{II}$ (day)
5797.64831	3033.0	I	0.00046	-0.00005	5797.25499	3031.5	II	0.00061	0.00011
5797.91059	3034.0	I	0.00042	-0.00008	5797.51730	3032.5	II	0.00060	0.00010
5798.17290	3035.0	I	0.00041	-0.00009	5797.77958	3033.5	II	0.00056	0.00006
5798.43522	3036.0	I	0.00042	-0.00008	5798.04192	3034.5	II	0.00059	0.00009
5798.69750	3037.0	I	0.00038	-0.00012	5798.30430	3035.5	II	0.00065	0.00015
5798.95987	3038.0	I	0.00044	-0.00007	5798.56658	3036.5	II	0.00061	0.00011
5799.22219	3039.0	I	0.00044	-0.00007	5798.82883	3037.5	II	0.00055	0.00004
5799.48450	3040.0	I	0.00042	-0.00008	5799.09109	3038.5	II	0.00049	-0.00001
5799.74680	3041.0	I	0.00041	-0.00009	5799.35343	3039.5	II	0.00052	0.00002
5800.00915	3042.0	I	0.00045	-0.00006	5799.61583	3040.5	II	0.00060	0.00010
5800.27136	3043.0	I	0.00033	-0.00017	5799.87847	3041.5	II	0.00092	0.00042
5800.53375	3044.0	I	0.00041	-0.00009	5800.14042	3042.5	II	0.00055	0.00005
5800.79601	3045.0	I	0.00035	-0.00015	5800.40276	3043.5	II	0.00058	0.00007
5801.05841	3046.0	I	0.00044	-0.00006	5800.66503	3044.5	II	0.00053	0.00003
5801.32068	3047.0	I	0.00039	-0.00011	5800.92739	3045.5	II	0.00058	0.00008
5801.58306	3048.0	I	0.00045	-0.00005	5801.18955	3046.5	II	0.00042	-0.00008
5801.84539	3049.0	I	0.00046	-0.00004	5801.45207	3047.5	II	0.00062	0.00012
5803.15703	3054.0	I	0.00052	0.00002	5801.71447	3048.5	II	0.00070	0.00020
5803.41922	3055.0	I	0.00040	-0.00010	5803.28830	3054.5	II	0.00064	0.00013
5803.68156	3056.0	I	0.00042	-0.00008	5803.55064	3055.5	II	0.00065	0.00015
5803.94397	3057.0	I	0.00051	0.00001	5803.81290	3056.5	II	0.00061	0.00010
5804.20622	3058.0	I	0.00044	-0.00006	5804.07518	3057.5	II	0.00056	0.00006
5804.46852	3059.0	I	0.00043	-0.00007	5804.33752	3058.5	II	0.00059	0.00009
5804.73098	3060.0	I	0.00057	0.00007	5804.59987	3059.5	II	0.00062	0.00012
5804.99308	3061.0	I	0.00036	-0.00015	5804.86217	3060.5	II	0.00060	0.00010
5805.25550	3062.0	I	0.00046	-0.00004	5805.12447	3061.5	II	0.00059	0.00008
5805.51784	3063.0	I	0.00048	-0.00002	5805.38688	3062.5	II	0.00068	0.00018
5805.78006	3064.0	I	0.00038	-0.00012	5805.64934	3063.5	II	0.00082	0.00032
5806.04238	3065.0	I	0.00039	-0.00011	5805.91151	3064.5	II	0.00068	0.00018
5806.30477	3066.0	I	0.00046	-0.00005	5806.17373	3065.5	II	0.00058	0.00008
5806.56712	3067.0	I	0.00050	-0.00001	5806.43608	3066.5	II	0.00062	0.00011
5806.82940	3068.0	I	0.00045	-0.00005	5806.69838	3067.5	II	0.00059	0.00009
5807.09167	3069.0	I	0.00041	-0.00009	5806.96067	3068.5	II	0.00057	0.00007
5807.35401	3070.0	I	0.00043	-0.00007	5807.22302	3069.5	II	0.00060	0.00010
5807.61627	3071.0	I	0.00038	-0.00012	5807.74772	3071.5	II	0.00067	0.00017
5807.87864	3072.0	I	0.00043	-0.00008	5808.00991	3072.5	II	0.00054	0.00004
5808.14096	3073.0	I	0.00043	-0.00007	5808.27221	3073.5	II	0.00053	0.00002
5808.40327	3074.0	I	0.00043	-0.00007	5808.53459	3074.5	II	0.00059	0.00009
5808.66558	3075.0	I	0.00042	-0.00008	5808.79695	3075.5	II	0.00063	0.00013
5808.92788	3076.0	I	0.00040	-0.00010	5809.05922	3076.5	II	0.00059	0.00008
5809.19021	3077.0	I	0.00042	-0.00008	5809.32162	3077.5	II	0.00067	0.00017
5809.71445	3079.0	I	0.00003	-0.00047	5809.58393	3078.5	II	0.00066	0.00016
5809.97705	3080.0	I	0.00030	-0.00020	5809.84621	3079.5	II	0.00063	0.00013
5810.23950	3081.0	I	0.00044	-0.00006	5810.10852	3080.5	II	0.00062	0.00012
5810.50178	3082.0	I	0.00040	-0.00010	5810.37081	3081.5	II	0.00059	0.00009
5810.76405	3083.0	I	0.00035	-0.00015	5810.63311	3082.5	II	0.00057	0.00007
5811.02640	3084.0	I	0.00039	-0.00011	5810.89550	3083.5	II	0.00064	0.00014
5811.28878	3085.0	I	0.00045	-0.00005	5811.15768	3084.5	II	0.00051	0.00001
5811.55104	3086.0	I	0.00040	-0.00010	5811.42012	3085.5	II	0.00063	0.00013
5811.81335	3087.0	I	0.00039	-0.00011	5811.68243	3086.5	II	0.00063	0.00013
5812.07572	3088.0	I	0.00044	-0.00006	5811.94482	3087.5	II	0.00070	0.00020
5812.33787	3089.0	I	0.00028	-0.00022	5812.20700	3088.5	II	0.00057	0.00007
5812.60016	3090.0	I	0.00025	-0.00025	5812.46930	3089.5	II	0.00055	0.00005
5812.86218	3091.0	I	-0.00004	-0.00055	5812.73176	3090.5	II	0.00069	0.00019

TABLE 1 (CONTINUED)

BJD (+24 50000)	E	Type	$(O - C)_I$ (day)	$(O - C)_{II}$ (day)	BJD (+24 50000)	E	Type	$(O - C)_I$ (day)	$(O - C)_{II}$ (day)
5813.12485	3092.0	I	0.00030	-0.00020	5812.99405	3091.5	II	0.00066	0.00016
5813.38697	3093.0	I	0.00010	-0.00040	5813.51857	3093.5	II	0.00055	0.00005
5813.64950	3094.0	I	0.00032	-0.00018	5813.78083	3094.5	II	0.00049	-0.00001
5813.91198	3095.0	I	0.00048	-0.00002	5814.04320	3095.5	II	0.00055	0.00005
5814.17418	3096.0	I	0.00037	-0.00013	5814.30553	3096.5	II	0.00056	0.00006
5814.43651	3097.0	I	0.00038	-0.00013	5814.56796	3097.5	II	0.00067	0.00017
5814.69876	3098.0	I	0.00031	-0.00019	5814.83014	3098.5	II	0.00054	0.00004
5814.96114	3099.0	I	0.00037	-0.00013	5815.09257	3099.5	II	0.00065	0.00015
5815.22344	3100.0	I	0.00036	-0.00014	5815.35425	3100.5	II	0.00001	-0.00049
5815.48564	3101.0	I	0.00024	-0.00026	5815.61713	3101.5	II	0.00057	0.00007
5815.74811	3102.0	I	0.00040	-0.00010	5815.87944	3102.5	II	0.00057	0.00007
5816.01052	3103.0	I	0.00049	-0.00001	5816.14174	3103.5	II	0.00055	0.00005
5816.27266	3104.0	I	0.00031	-0.00019	5816.40395	3104.5	II	0.00044	-0.00006
5816.53504	3105.0	I	0.00037	-0.00013	5816.66593	3105.5	II	0.00010	-0.00040
5816.79728	3106.0	I	0.00030	-0.00020	5816.92880	3106.5	II	0.00066	0.00016
5817.05964	3107.0	I	0.00034	-0.00016	5817.19100	3107.5	II	0.00054	0.00004
5817.32198	3108.0	I	0.00037	-0.00013	5817.45352	3108.5	II	0.00075	0.00025
5817.58428	3109.0	I	0.00035	-0.00015	5817.71574	3109.5	II	0.00065	0.00015
5817.84666	3110.0	I	0.00041	-0.00009	5817.97813	3110.5	II	0.00073	0.00023
5818.10956	3111.0	I	0.00100	0.00050	5818.24076	3111.5	II	0.00104	0.00054
5818.37127	3112.0	I	0.00039	-0.00011	5818.50250	3112.5	II	0.00046	-0.00004
5818.63346	3113.0	I	0.00026	-0.00024	5818.76494	3113.5	II	0.00058	0.00008
5818.89586	3114.0	I	0.00034	-0.00016	5819.02721	3114.5	II	0.00054	0.00004
5819.15825	3115.0	I	0.00041	-0.00009	5819.28957	3115.5	II	0.00058	0.00008
5819.42062	3116.0	I	0.00047	-0.00003	5819.55194	3116.5	II	0.00063	0.00013
5819.68287	3117.0	I	0.00040	-0.00010	5819.81412	3117.5	II	0.00050	0.00000
5819.94514	3118.0	I	0.00036	-0.00014	5820.07665	3118.5	II	0.00071	0.00021
5820.20747	3119.0	I	0.00037	-0.00013	5820.33886	3119.5	II	0.00061	0.00011
5820.46980	3120.0	I	0.00038	-0.00012	5820.60122	3120.5	II	0.00064	0.00014
5820.73204	3121.0	I	0.00031	-0.00019	5820.86365	3121.5	II	0.00076	0.00026
5820.99433	3122.0	I	0.00028	-0.00022	5821.12575	3122.5	II	0.00054	0.00004
5821.25663	3123.0	I	0.00026	-0.00024	5821.38816	3123.5	II	0.00064	0.00014
5821.51917	3124.0	I	0.00049	-0.00001	5821.65047	3124.5	II	0.00063	0.00013
5821.78135	3125.0	I	0.00035	-0.00015	5821.91268	3125.5	II	0.00052	0.00002
5822.04365	3126.0	I	0.00033	-0.00017	5822.17504	3126.5	II	0.00057	0.00007
5822.30599	3127.0	I	0.00036	-0.00014	5822.43737	3127.5	II	0.00058	0.00008
5822.56831	3128.0	I	0.00036	-0.00014	5822.69969	3128.5	II	0.00058	0.00008
5822.83056	3129.0	I	0.00029	-0.00021	5822.96218	3129.5	II	0.00075	0.00025
5823.09302	3130.0	I	0.00044	-0.00006	5823.22431	3130.5	II	0.00057	0.00007
5823.35536	3131.0	I	0.00046	-0.00004	5823.48652	3131.5	II	0.00046	-0.00004
5823.61756	3132.0	I	0.00034	-0.00016	5823.74905	3132.5	II	0.00067	0.00018
5823.88003	3133.0	I	0.00049	-0.00001	5824.01127	3133.5	II	0.00058	0.00008
5824.14225	3134.0	I	0.00040	-0.00010	5824.27361	3134.5	II	0.00060	0.00010
5824.40453	3135.0	I	0.00036	-0.00014	5824.53601	3135.5	II	0.00068	0.00018
5824.66695	3136.0	I	0.00047	-0.00003	5824.79824	3136.5	II	0.00060	0.00010
5824.92924	3137.0	I	0.00044	-0.00006	5825.06050	3137.5	II	0.00054	0.00004
5825.19154	3138.0	I	0.00043	-0.00007	5825.32279	3138.5	II	0.00051	0.00001
5825.45390	3139.0	I	0.00046	-0.00003	5825.58529	3139.5	II	0.00070	0.00020
5825.71621	3140.0	I	0.00046	-0.00004	5825.84753	3140.5	II	0.00062	0.00012
5825.97848	3141.0	I	0.00041	-0.00009	5826.10994	3141.5	II	0.00071	0.00021
5826.24082	3142.0	I	0.00043	-0.00006	5826.37214	3142.5	II	0.00060	0.00010
5826.50316	3143.0	I	0.00045	-0.00005	5826.63450	3143.5	II	0.00063	0.00014
5826.76539	3144.0	I	0.00037	-0.00013	5826.89681	3144.5	II	0.00063	0.00013
5827.02783	3145.0	I	0.00049	-0.00001	5827.15911	3145.5	II	0.00062	0.00012

TABLE 1 (CONTINUED)

BJD (+24 50000)	E	Type	$(O - C)_I$ (day)	$(O - C)_{II}$ (day)	BJD (+24 50000)	E	Type	$(O - C)_I$ (day)	$(O - C)_{II}$ (day)
5827.29006	3146.0	I	0.00041	-0.00009	5827.42147	3146.5	II	0.00066	0.00016
5827.55248	3147.0	I	0.00051	0.00001	5827.68367	3147.5	II	0.00054	0.00005
5827.81476	3148.0	I	0.00048	-0.00002	5827.94613	3148.5	II	0.00069	0.00019
5828.07705	3149.0	I	0.00044	-0.00005	5828.20842	3149.5	II	0.00066	0.00016
5828.33942	3150.0	I	0.00050	0.00000	5828.47068	3150.5	II	0.00060	0.00010
5828.60162	3151.0	I	0.00038	-0.00012	5828.73306	3151.5	II	0.00066	0.00016
5828.86430	3152.0	I	0.00074	0.00024	5828.99522	3152.5	II	0.00051	0.00001
5829.12629	3153.0	I	0.00042	-0.00008	5829.25755	3153.5	II	0.00052	0.00003
5829.38866	3154.0	I	0.00047	-0.00003	5829.51981	3154.5	II	0.00046	-0.00004
5829.65093	3155.0	I	0.00043	-0.00007	5829.78236	3155.5	II	0.00069	0.00020
5829.91329	3156.0	I	0.00047	-0.00003	5830.04457	3156.5	II	0.00059	0.00009
5830.17562	3157.0	I	0.00048	-0.00002	5830.30680	3157.5	II	0.00051	0.00001
5830.43787	3158.0	I	0.00042	-0.00008	5830.56913	3158.5	II	0.00051	0.00002
5830.70019	3159.0	I	0.00042	-0.00008	5830.83157	3159.5	II	0.00064	0.00014
5830.96248	3160.0	I	0.00039	-0.00011	5831.09376	3160.5	II	0.00052	0.00002
5831.22489	3161.0	I	0.00049	-0.00001	5831.35620	3161.5	II	0.00064	0.00014
5831.48711	3162.0	I	0.00039	-0.00011	5831.61846	3162.5	II	0.00058	0.00008
5831.74944	3163.0	I	0.00040	-0.00010	5831.88079	3163.5	II	0.00059	0.00009
5832.01179	3164.0	I	0.00044	-0.00006	5832.14315	3164.5	II	0.00064	0.00014
5832.27407	3165.0	I	0.00039	-0.00010	5832.40538	3165.5	II	0.00055	0.00005
5832.53641	3166.0	I	0.00042	-0.00007	5832.66774	3166.5	II	0.00059	0.00010
5832.79871	3167.0	I	0.00041	-0.00009	5832.92998	3167.5	II	0.00052	0.00002

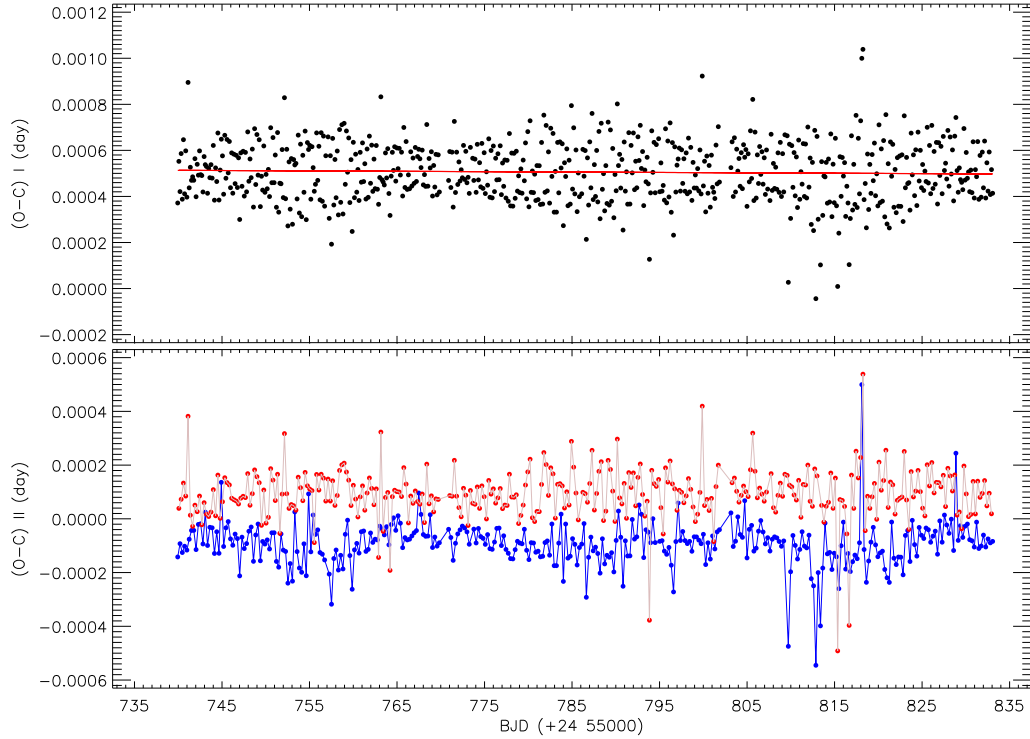


Fig. 2. The variations of time of minimum residuals of $(O - C)_I$ and $(O - C)_{II}$ obtained by applying a linear correction. In the bottom panel, the filled blue circles represent the primary minima; the filled red circles represent the secondary minima. In the upper panel all the residuals are plotted with filled black circles, while the red line represents a linear fit. The color figure can be viewed online.

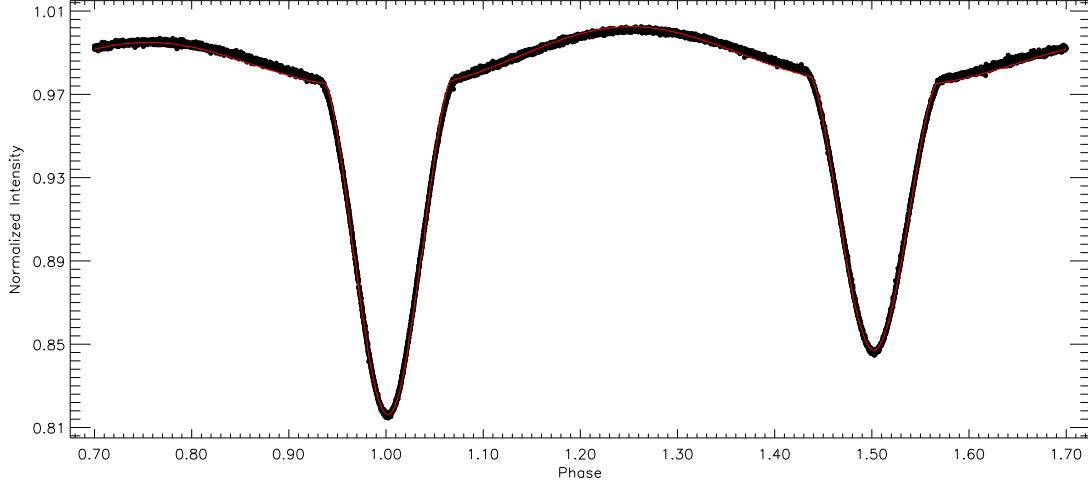


Fig. 3. The light curve along the orbital cycle, from BJD 2455739.94 to 2455829.13. In the figure, the filled circles represent the observations, while the red smooth line represents the synthetic light curve. The color figure can be viewed online.

were tried in the light curve analyses, astrophysically acceptable parameters were obtained only for the detached system mode.

The PHOEBE V.0.32, needs a temperature value for the primary component. We determined its temperature from the *JHK* brightness given by Cutri et al. (2003). The de-reddened colors were found to be $(H - K)_0 = 0^m.252$ and $(J - K)_0 = 0^m.629$. Then a temperature value of 4220 ± 20 K corresponding to the de-reddened colours was obtained by using the calibrations given by Tokunaga (2000). We accepted this value as the primary component temperature. The temperature of the secondary component was taken as an adjustable free parameter. In the analyses, some coefficients, such as the albedos (A_1 and A_2), the gravity-darkening coefficients (g_1 and g_2) and the limb-darkening coefficients (x_1 and x_2), were taken from the tables given by Lucy (1967); Rucinski (1969); Van Hamme (1993), considering the possible temperatures of both components. The rest of the parameters, such as the dimensionless potentials (Ω_1 and Ω_2), the fractional luminosity (L_1) of the primary component, the inclination (i) and the mass ratio (q) of the system, were taken as adjustable free parameters.

The computed values of the free parameters are tabulated in Table 2, while the synthetic light curve derived by these parameters is shown in Figure 3. As the table shows, some errors are smaller than the expected values. However, the errors given in the table were computed by the PHOEBE V.0.32, depending on Taylor (1997). In fact the χ^2 was computed as 3.15×10^{-3} from the Kepler short cadence data. The

3D model of Roche geometry obtained with these parameters is shown in Figure 4.

It should be noted that we obtained a solution after some iterations in the detached system mode of the Wilson-Devinney Code (Wilson & Devinney 1971; Wilson 1990). Although the synthetic curve fitted the observations very well, it was revealed that it did not fit the observations around phase 0.27. To solve this mismatched part of synthetic light curve, we assumed that there is a spotted area on a component, considering the flare activity. We assumed that the spotted area was on the primary component. It could be assumed that the spotted star was the secondary component, which would lead to another acceptable solution.

The $(B - V)$ color indexes were computed as $1^m.233$ and $1^m.329$ for the primary and secondary components, respectively. The computed color indexes are in agreement with the values found by Walkowicz & Basri (2013). Considering these values, we determined the masses as $0.644M_\odot$ and $0.570M_\odot$ for primary and secondary components. Then, the semi-major axis of the system was found to be $1.84R_\odot$ (0.0086 AU) according to Kepler's third law. With this value for the semi-major axis, the radius of the primary component was found to be $0.701R_\odot$, while that of the secondary was $0.650R_\odot$.

2.3. Flare Activity and the OPEA Model

The main subject of this paper is about flare activity in KIC 12004834. To demonstrate the nature of the flare activity occurring in a star with

TABLE 2
PARAMETERS OBTAINED FROM THE LIGHT CURVE ANALYSIS OF KIC 12004834

Parameter	Value
q	0.743 ± 0.001
i ($^{\circ}$)	75.89 ± 0.03
T_1 (K)	4220 (fixed)
T_2 (K)	4001 ± 11
Ω_1	4.308 ± 0.004
Ω_2	5.485 ± 0.007
L_1/L_2	0.245 ± 0.067
g_1, g_2	0.32 (fixed)
A_1, A_2	0.32 (fixed)
$x_{1,bol}, x_{2,bol}$	0.377, 0.001 (fixed)
x_1, x_2	0.369, 0.001 (fixed)
$< r_1 >$	0.287 ± 0.001
$< r_2 >$	0.172 ± 0.001
$Co - Lat_{Spot}^{(rad)}$	1.920 ± 0.004
$Long_{Spot}^{(rad)}$	1.710 ± 0.002
$R_{Spot}^{(rad)}$	0.244 ± 0.003
T_{fSpot}	0.960 ± 0.001

known photometric data, Dal & Evren (2010) and Dal (2012) described a simple way depending on the method mentioned by Gershberg (1972), which is just a smoothing out of the flares. However, apart from the flare activity, the light curve of KIC 12004834 exhibits other effects caused by both the geometrical nature of the components and the structures on them, such as eclipses and cool spots.

In order to determine and analyze the flares, first we removed the variations seen out-of-flares in the light curves. We follow the method of Dal & Evren (2010) for KIC 12004834. For this purpose, using the synthetic light curve derived from the light curve analyses described in the previous section, the residual data were obtained as a pre-whitened light curve, in which there was only flare activity variation. Following Dal (2012), 149 flares were detected from the available short cadence data. In the analyses, the synthetic light curve allowed us to fix the quiescent levels at the flare moment, which are shown in Figure 5.

Taking into account that the luminosity parameter enters in the energy calculations as described by Dal & Evren (2010, 2011), the equivalent duration parameter was computed for each flare, instead of its energy. According to the beginning and the end of a

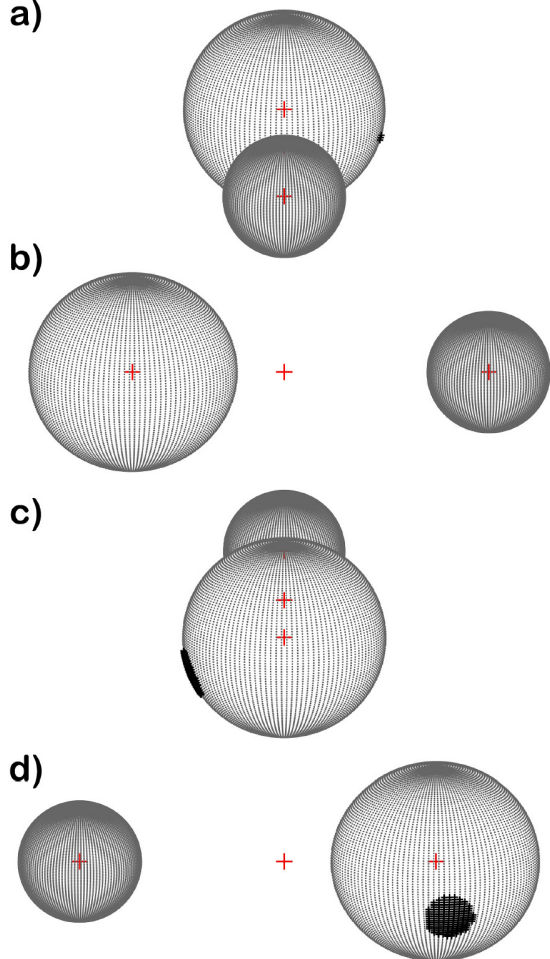


Fig. 4. The 3D model of Roche geometry and spotted area distribution derived from the light curve analysis is shown for different phases, such as (a) 0.00, (b) 0.25, (c) 0.50, (d) 0.75. The color figure can be viewed online.

flare, the desired parameters, such as flare rise times (T_r), decay times (T_d), amplitudes of flare maxima, flare equivalent durations (P), were computed for each flare. The flare equivalent durations were computed by equation (2) taken from Gershberg (1972):

$$P = \int [(I_{flare} - I_0)/I_0] dt \quad (2)$$

where I_0 is the flux of the star in the quiet state. As described above, the synthetic light curve derived by the light curve analysis was taken as I_0 . I_{flare} is the intensity observed at the moment of the flare. P is the flare-equivalent duration in the observing band. All the computed parameters are listed in Table 3 for these 149 flares. The general standard errors were

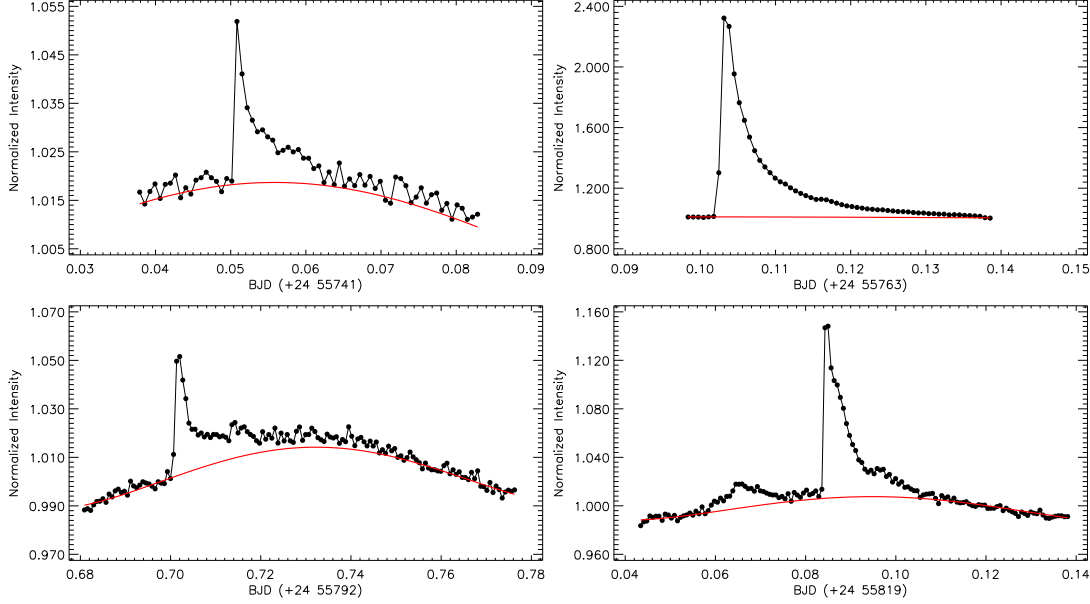


Fig. 5. Four different samples for the flare light variations are shown. In the figure, the filled circles represent the observations, while the (red) lines represent the synthetic light curve obtained from the light curve analysis, which was taken as the quiescent levels for each flare. The color figure can be viewed online.

computed by using the methods described by Taylor (1997) for the time scales such as flare rise and decay times.

The distributions of flare equivalent durations on a logarithmic scale versus flare total durations were modelled by the One Phase Exponential Association (hereafter OPEA) defined by equation (3), using the SPSS V17.0 (Green et al. 1999) and GrahpPad Prism V5.02 (Dawson & Trapp 2004) software:

$$y = y_0 + (\text{Plateau} - y_0) \times (1 - e^{-k \times x}) \quad (3)$$

where y is the flare equivalent duration, x is the flare total duration. According to the description of Dal & Evren (2010), the most important parameter in this equation is the *Plateau* term to reveal the flare behavior of a star. Following three different methods described by D'Agostino & Stephens (1986), the probability values (*p-value*) were calculated to test the quality of the fit. The *p-value* was found to be < 0.001 in all the methods. The derived OPEA model is shown in Figure 6 together with the observed flare equivalent durations. The parameters computed from the model are listed in Table 4.

In contrast to the known UV Ceti flare stars, KIC 12004834 is a binary system. It is well known that the flare events are generally random phenomena. To test this situation for a close binary like KIC 12004834, we calculated the phase distribution of the flares, depending on the orbital period of the

system. The phase distribution is shown in Figure 7. In the figure, the distribution of the total number of flares computed in phase intervals of 0.05, for all 149 flares is shown.

We also derived the flare energy spectrum (Gershberg 1972) for KIC 12004834. Like for the OPEA model, we again used the flare equivalent duration instead of the flare energy. To derive the flare energy spectrum, the cumulative flare frequencies were computed for 149 flares, and then, its distribution was derived in order to compare KIC 12004834 to its analogues. The obtained cumulative flare frequency distribution and its models are shown in Figure 8.

In the literature there are two other flare frequency descriptions. Contrary to Gershberg (1972), Ishida et al. (1991) described the flare frequencies N_1 and N_2 , a flare number and a total flare-equivalent duration emitting per hour, respectively. In this study, we detected 149 flares from the available observations lasting 89.19 days. We computed the frequencies by equations (4) and (5) (Ishida et al. 1991):

$$N_1 = \Sigma n_f / \Sigma DT \quad (4)$$

$$N_2 = \Sigma P / \Sigma DT \quad (5)$$

where Σn_f is the total flare number, ΣDT is the total observing duration, and ΣP is the total equivalent duration. We found that the N_1 frequency is 0.070 h^{-1} , while the N_2 frequency is 0.62 second/hour for KIC 12004834. It should be noted that

TABLE 3

THE FLARE PARAMETERS COMPUTED FROM KIC 12004834'S THE AVAILABLE SHORT CADENCE DATA IN THE KEPLER MISSION DATABASE

T _{max} (BJD-2450000)	P (s)	T _r (s)	T _d (s)	T _t (s)	Amplitude (Relative Flux)
55806.51506	0.762	58.846 ± 3.616	58.846 ± 3.616	117.692 ± 5.114	0.01180
55804.54459	0.471	58.846 ± 3.616	58.847 ± 3.616	117.693 ± 5.114	0.01221
55811.74873	0.896	58.847 ± 3.616	58.846 ± 3.616	117.693 ± 5.114	0.01720
55766.08239	0.745	58.848 ± 3.616	117.686 ± 5.114	176.534 ± 6.264	0.00989
55830.23880	1.240	58.845 ± 3.616	176.538 ± 6.264	235.383 ± 7.233	0.01713
55801.66075	1.066	117.702 ± 5.114	117.685 ± 5.114	235.386 ± 7.233	0.00827
55794.32581	1.117	58.855 ± 3.617	176.532 ± 6.263	235.387 ± 7.233	0.00929
55831.45798	1.880	117.700 ± 5.114	117.692 ± 5.114	235.392 ± 7.233	0.01391
55822.77794	1.137	58.846 ± 3.616	176.546 ± 6.264	235.392 ± 7.233	0.01338
55801.95704	2.098	58.846 ± 3.616	235.386 ± 7.233	294.233 ± 8.086	0.01416
55804.71215	1.290	117.684 ± 5.114	176.549 ± 6.264	294.233 ± 8.086	0.01001
55823.82889	1.051	58.846 ± 3.616	235.393 ± 7.233	294.240 ± 8.086	0.01032
55822.73912	1.633	117.692 ± 5.114	235.384 ± 7.233	353.076 ± 8.858	0.01343
55760.03465	0.632	58.848 ± 3.616	294.239 ± 8.086	353.087 ± 8.858	0.01071
55801.75679	2.621	58.838 ± 3.616	294.251 ± 8.087	353.088 ± 8.858	0.01381
55799.55611	1.312	117.702 ± 5.114	235.387 ± 7.233	353.089 ± 8.858	0.00642
55780.13399	1.711	117.703 ± 5.114	235.389 ± 7.233	353.092 ± 8.858	0.01102
55766.07149	0.848	117.704 ± 5.114	235.391 ± 7.233	353.094 ± 8.858	0.01050
55768.37983	2.922	58.857 ± 3.617	294.255 ± 8.087	353.112 ± 8.858	0.01705
55756.03029	1.168	117.687 ± 5.114	294.257 ± 8.087	411.944 ± 9.568	0.00935
55756.56293	1.245	117.696 ± 5.114	294.248 ± 8.086	411.944 ± 9.568	0.01079
55740.56791	2.973	117.696 ± 5.114	294.251 ± 8.087	411.947 ± 9.568	0.01556
55831.96472	4.468	58.846 ± 3.616	411.929 ± 9.568	470.775 ± 10.228	0.03456
55778.12332	2.165	117.694 ± 5.114	353.093 ± 8.858	470.787 ± 10.229	0.01238
55776.73927	1.898	117.695 ± 5.114	353.093 ± 8.858	470.788 ± 10.229	0.00963
55792.90704	6.883	117.694 ± 5.114	411.937 ± 9.568	529.631 ± 10.849	0.02718
55779.79002	9.266	117.694 ± 5.114	411.940 ± 9.568	529.634 ± 10.849	0.04237
55755.22928	3.861	176.552 ± 6.264	353.087 ± 8.858	529.640 ± 10.849	0.01210
55772.93588	0.849	117.704 ± 5.114	411.941 ± 9.568	529.644 ± 10.849	0.01032
55761.90026	1.219	117.704 ± 5.114	411.943 ± 9.568	529.648 ± 10.849	0.01217
55755.87908	1.132	294.248 ± 8.086	235.400 ± 7.233	529.648 ± 10.849	0.00573
55783.26307	0.793	58.856 ± 3.617	470.794 ± 10.229	529.650 ± 10.849	0.00322
55762.79935	1.244	117.704 ± 5.114	411.952 ± 9.568	529.655 ± 10.849	0.01132
55766.10282	2.214	294.247 ± 8.086	294.238 ± 8.086	588.485 ± 11.436	0.01453
55792.98265	2.377	117.693 ± 5.114	470.793 ± 10.229	588.486 ± 11.436	0.01164
55825.24424	2.172	117.700 ± 5.114	470.786 ± 10.229	588.486 ± 11.436	0.01260
55810.05753	1.166	176.557 ± 6.264	411.933 ± 9.568	588.489 ± 11.436	0.01357
55742.47985	1.287	176.545 ± 6.264	411.946 ± 9.568	588.490 ± 11.436	0.01300
55747.50593	1.506	117.696 ± 5.114	470.802 ± 10.229	588.498 ± 11.436	0.01536
55742.24282	3.543	294.241 ± 8.086	294.259 ± 8.087	588.500 ± 11.436	0.01447
55829.60128	2.781	117.692 ± 5.114	529.629 ± 10.849	647.322 ± 11.994	0.01256
55826.06293	3.057	176.546 ± 6.264	470.776 ± 10.228	647.323 ± 11.994	0.00379
55792.31311	1.336	176.540 ± 6.264	470.793 ± 10.229	647.333 ± 11.994	0.00897
55762.79186	3.297	117.686 ± 5.114	529.648 ± 10.849	647.334 ± 11.994	0.01830
55779.32482	2.116	117.703 ± 5.114	529.635 ± 10.849	647.337 ± 11.994	0.01469
55748.36688	1.896	235.392 ± 7.233	411.963 ± 9.568	647.355 ± 11.994	0.01075
55776.23933	3.682	117.694 ± 5.114	588.491 ± 11.436	706.185 ± 12.527	0.00924
55796.02792	3.817	117.703 ± 5.114	588.485 ± 11.436	706.188 ± 12.527	0.01597
55765.69482	5.587	235.408 ± 7.233	470.789 ± 10.229	706.197 ± 12.528	0.01827
55763.59627	1.525	117.704 ± 5.114	588.495 ± 11.436	706.199 ± 12.528	0.00532
55811.84817	9.222	176.539 ± 6.264	588.481 ± 11.436	765.020 ± 13.039	0.02482

TABLE 3 (CONTINUED)

T _{max} (BJD-2450000)	P (s)	T _r (s)	T _d (s)	T _t (s)	Amplitude (Relative Flux)
55808.84242	3.326	176.548 ± 6.264	588.472 ± 11.436	765.020 ± 13.039	0.01629
55806.89444	2.641	294.241 ± 8.086	470.781 ± 10.229	765.022 ± 13.039	0.04012
55810.38923	3.032	176.548 ± 6.264	588.481 ± 11.436	765.029 ± 13.039	0.00910
55779.65108	6.755	176.551 ± 6.264	588.481 ± 11.436	765.031 ± 13.039	0.02747
55777.26170	2.436	58.847 ± 3.616	706.185 ± 12.527	765.032 ± 13.039	0.01427
55800.70583	1.053	176.549 ± 6.264	588.483 ± 11.436	765.032 ± 13.039	0.01235
55773.50393	2.461	235.407 ± 7.233	529.627 ± 10.849	765.034 ± 13.039	0.04477
55762.69582	2.510	58.839 ± 3.616	706.199 ± 12.528	765.038 ± 13.039	0.01041
55748.38868	3.771	117.704 ± 5.114	647.337 ± 11.994	765.042 ± 13.039	0.01522
55746.66405	1.236	117.704 ± 5.114	647.338 ± 11.994	765.043 ± 13.039	0.01060
55743.15553	2.308	353.098 ± 8.858	411.946 ± 9.568	765.043 ± 13.039	0.01575
55745.65597	2.618	117.705 ± 5.114	647.347 ± 11.994	765.052 ± 13.039	0.01126
55821.60644	2.042	294.230 ± 8.086	529.632 ± 10.849	823.862 ± 13.531	0.00904
55798.75171	4.518	58.838 ± 3.616	765.032 ± 13.039	823.871 ± 13.531	0.02078
55794.34352	4.924	58.856 ± 3.617	765.026 ± 13.039	823.882 ± 13.531	0.01618
55783.25353	3.925	235.388 ± 7.233	588.498 ± 11.436	823.886 ± 13.531	0.01514
55763.58673	4.125	176.551 ± 6.264	647.342 ± 11.994	823.893 ± 13.531	0.01013
55775.11139	3.272	117.704 ± 5.114	706.194 ± 12.528	823.897 ± 13.531	0.01310
55740.48481	2.590	294.250 ± 8.087	529.652 ± 10.849	823.902 ± 13.531	0.01744
55747.88464	3.972	58.857 ± 3.617	765.051 ± 13.039	823.908 ± 13.531	0.02227
55820.70669	11.448	176.546 ± 6.264	706.171 ± 12.527	882.717 ± 14.006	0.02987
55812.88346	5.447	58.855 ± 3.617	823.865 ± 13.531	882.720 ± 14.006	0.02041
55792.81781	3.461	411.937 ± 9.568	470.783 ± 10.229	882.720 ± 14.006	0.01339
55809.54465	3.030	117.693 ± 5.114	765.029 ± 13.039	882.722 ± 14.006	0.01444
55807.14032	3.450	411.934 ± 9.568	470.789 ± 10.229	882.723 ± 14.006	0.01147
55815.95868	2.639	58.856 ± 3.617	823.872 ± 13.531	882.728 ± 14.006	0.01146
55744.32436	4.279	176.553 ± 6.264	706.196 ± 12.528	882.749 ± 14.006	0.01569
55742.23055	5.768	117.705 ± 5.114	765.052 ± 13.039	882.757 ± 14.006	0.01393
55817.51569	6.776	117.701 ± 5.114	823.864 ± 13.531	941.565 ± 14.465	0.02661
55792.21979	1.686	176.541 ± 6.264	765.026 ± 13.039	941.567 ± 14.465	0.00954
55806.74527	3.401	176.548 ± 6.264	765.021 ± 13.039	941.569 ± 14.465	0.01014
55804.56094	2.295	176.539 ± 6.264	765.031 ± 13.039	941.571 ± 14.465	0.00944
55743.93339	1.965	176.553 ± 6.264	765.043 ± 13.039	941.597 ± 14.466	0.00956
55818.95147	5.622	58.846 ± 3.616	941.564 ± 14.465	1000.410 ± 14.911	0.02512
55820.43834	4.285	117.701 ± 5.114	882.718 ± 14.006	1000.419 ± 14.911	0.00997
55800.59413	2.617	117.702 ± 5.114	882.725 ± 14.006	1000.427 ± 14.911	0.01204
55773.99094	2.775	58.848 ± 3.616	941.585 ± 14.465	1000.433 ± 14.911	0.01211
55760.96984	3.584	117.696 ± 5.114	882.743 ± 14.006	1000.439 ± 14.911	0.01461
55777.94827	9.265	176.542 ± 6.264	823.897 ± 13.531	1000.439 ± 14.911	0.02508
55756.66238	4.502	176.552 ± 6.264	823.888 ± 13.531	1000.440 ± 14.911	0.01090
55755.86341	3.832	176.552 ± 6.264	823.897 ± 13.531	1000.449 ± 14.911	0.00772
55752.17713	3.504	176.553 ± 6.264	823.897 ± 13.531	1000.451 ± 14.911	0.01063
55803.99153	3.654	294.233 ± 8.086	765.022 ± 13.039	1059.254 ± 15.343	0.01084
55826.07315	3.786	176.546 ± 6.264	882.715 ± 14.006	1059.261 ± 15.343	0.00801
55741.05083	10.207	58.849 ± 3.616	1000.455 ± 14.911	1059.304 ± 15.343	0.03355
55805.48113	6.780	235.386 ± 7.233	882.724 ± 14.006	1118.109 ± 15.763	0.01629
55792.62642	8.534	353.090 ± 8.858	765.027 ± 13.039	1118.117 ± 15.763	0.02378
55751.93397	6.862	117.696 ± 5.114	1000.442 ± 14.911	1118.138 ± 15.763	0.03174
55765.32020	4.999	176.551 ± 6.264	941.589 ± 14.466	1118.140 ± 15.763	0.01279
55807.98013	4.321	117.702 ± 5.114	1059.261 ± 15.343	1176.963 ± 16.173	0.01249
55792.84574	5.480	176.549 ± 6.264	1000.423 ± 14.911	1176.972 ± 16.173	0.02244
55804.36682	5.572	235.386 ± 7.233	1000.417 ± 14.911	1235.803 ± 16.572	0.01366
55818.06535	18.899	117.692 ± 5.114	1118.111 ± 15.763	1235.803 ± 16.572	0.04024
55763.74271	5.420	235.399 ± 7.233	1000.445 ± 14.911	1235.845 ± 16.572	0.01580

TABLE 3 (CONTINUED)

Tmax (BJD-2450000)	P (s)	T_r (s)	T_d (s)	T_t (s)	Amplitude (Relative Flux)
55808.48143	6.886	294.241 \pm 8.086	1000.415 \pm 14.911	1294.656 \pm 16.962	0.01014
55752.86099	2.487	470.793 \pm 10.229	823.897 \pm 13.531	1294.690 \pm 16.962	0.01033
55748.43023	6.680	176.536 \pm 6.264	1118.157 \pm 15.764	1294.693 \pm 16.962	0.01774
55757.40209	13.431	235.400 \pm 7.233	1059.296 \pm 15.343	1294.696 \pm 16.962	0.02852
55740.24641	5.290	176.554 \pm 6.264	1118.152 \pm 15.764	1294.706 \pm 16.962	0.01038
55755.23405	7.243	58.857 \pm 3.617	1235.850 \pm 16.572	1294.707 \pm 16.962	0.02040
55799.53567	5.955	58.847 \pm 3.616	1294.670 \pm 16.962	1353.517 \pm 17.343	0.02091
55759.69340	8.248	235.400 \pm 7.233	1118.134 \pm 15.763	1353.535 \pm 17.344	0.01900
55748.56237	5.839	235.400 \pm 7.233	1118.140 \pm 15.763	1353.540 \pm 17.344	0.01245
55746.72876	6.982	294.240 \pm 8.086	1059.301 \pm 15.343	1353.542 \pm 17.344	0.01395
55759.69340	2.293	235.391 \pm 7.233	1118.152 \pm 15.764	1353.542 \pm 17.344	0.00198
55820.42199	10.170	176.539 \pm 6.264	1235.811 \pm 16.572	1412.350 \pm 17.716	0.01346
55797.44873	4.053	235.396 \pm 7.233	1176.969 \pm 16.173	1412.365 \pm 17.716	0.01008
55807.03611	20.538	294.241 \pm 8.086	1176.964 \pm 16.173	1471.205 \pm 18.082	0.03700
55791.63812	11.512	294.243 \pm 8.086	1176.973 \pm 16.173	1471.216 \pm 18.082	0.02267
55746.15729	4.354	117.697 \pm 5.114	1353.550 \pm 17.344	1471.247 \pm 18.082	0.01144
55806.00150	11.359	176.540 \pm 6.264	1412.367 \pm 17.716	1588.907 \pm 18.791	0.02162
55787.89945	7.928	58.847 \pm 3.616	1530.075 \pm 18.440	1588.922 \pm 18.791	0.00838
55768.84435	5.401	235.391 \pm 7.233	1353.537 \pm 17.344	1588.928 \pm 18.791	0.01316
55833.09059	25.717	117.700 \pm 5.114	1530.033 \pm 18.440	1647.734 \pm 19.136	0.07710
55819.06454	16.793	588.478 \pm 11.436	1059.265 \pm 15.343	1647.743 \pm 19.136	0.02017
55766.87590	18.093	235.391 \pm 7.233	1412.386 \pm 17.717	1647.777 \pm 19.136	0.03545
55773.95416	4.012	176.543 \pm 6.264	1471.237 \pm 18.082	1647.780 \pm 19.136	0.01109
55790.05588	38.271	411.947 \pm 9.568	1294.676 \pm 16.962	1706.623 \pm 19.475	0.16402
55816.58802	7.120	176.547 \pm 6.264	1588.891 \pm 18.791	1765.438 \pm 19.807	0.01858
55793.88104	24.987	117.702 \pm 5.114	1647.764 \pm 19.136	1765.466 \pm 19.808	0.11313
55826.02002	6.115	117.691 \pm 5.114	1706.585 \pm 19.475	1824.276 \pm 20.135	0.01318
55827.89170	10.892	117.691 \pm 5.114	1765.429 \pm 19.807	1883.121 \pm 20.457	0.02212
55819.08497	46.875	176.547 \pm 6.264	1765.435 \pm 19.807	1941.983 \pm 20.774	0.14180
55780.39486	10.869	588.489 \pm 11.436	1471.224 \pm 18.082	2059.714 \pm 21.395	0.01187
55765.45575	21.704	176.544 \pm 6.264	1883.185 \pm 20.457	2059.728 \pm 21.395	0.04175
55822.75342	10.331	353.085 \pm 8.858	2000.826 \pm 21.087	2353.911 \pm 22.872	0.01707
55828.63411	32.706	117.700 \pm 5.114	2412.751 \pm 23.156	2530.451 \pm 23.714	0.04817
55821.43071	23.129	294.240 \pm 8.086	2589.304 \pm 23.988	2883.544 \pm 25.314	0.01867
55756.89805	22.867	117.704 \pm 5.114	2765.928 \pm 24.793	2883.633 \pm 25.315	0.03313
55763.10313	119.328	117.704 \pm 5.114	2942.472 \pm 25.572	3060.177 \pm 26.078	1.31184
55764.80868	19.131	1059.301 \pm 15.343	2059.729 \pm 21.395	3119.030 \pm 26.328	0.01630
55810.14130	28.083	176.548 \pm 6.264	3118.961 \pm 26.327	3295.509 \pm 27.062	0.02015
55795.62606	59.471	117.703 \pm 5.114	3236.660 \pm 26.820	3354.362 \pm 27.303	0.05526
55822.11727	32.769	235.392 \pm 7.233	3177.782 \pm 26.575	3413.175 \pm 27.541	0.02822
55795.07436	37.409	353.089 \pm 8.858	3589.768 \pm 28.245	3942.857 \pm 29.601	0.04263
55792.70202	36.928	176.541 \pm 6.264	3766.321 \pm 28.931	3942.862 \pm 29.601	0.04881
55766.71856	117.197	235.391 \pm 7.233	4119.463 \pm 30.257	4354.854 \pm 31.109	0.11637
55741.94107	52.968	1059.303 \pm 15.343	4296.050 \pm 30.899	5355.353 \pm 34.498	0.02498

the N_2 frequency is a unitless parameter, because the unit of ΣDT is time as well as the unit of ΣDT . However, the N_2 frequency is given in units of second/hour to facilitate the reading of the manuscript.

3. RESULTS AND DISCUSSION

We analysed the light curve and $(O - C)$ residuals of the system for the first time in the literature. The mass ratio of the system (q) was found

to be 0.743 ± 0.001 , while the inclination (i) was found to be $75^\circ.89 \pm 0^\circ.03$. This inclination (i) value is in agreement with the inclination (i) value of $72^\circ.47$ given by Coughlin et al. (2011). The mass of the primary component was found to be $0.64M_\odot$ with a radius of $0.70R_\odot$, while it was found to be $0.57M_\odot$ for the secondary component with a radius of $0.65R_\odot$. Although these parameters are a bit larger than those found by Coughlin et al. (2011),

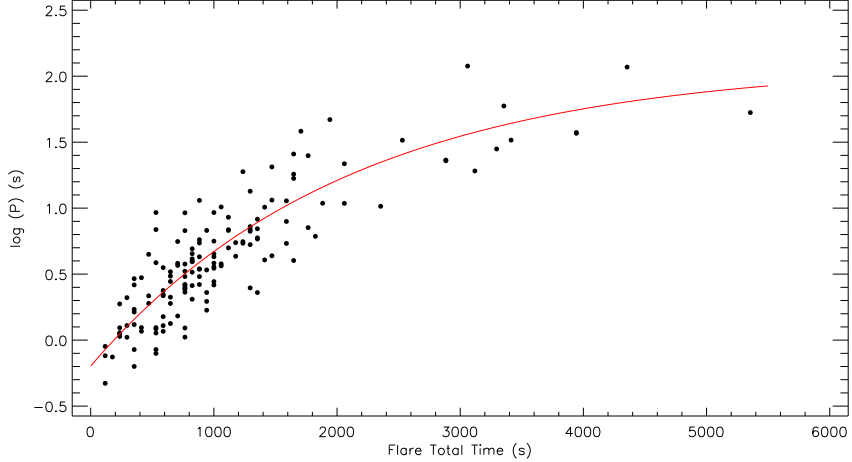


Fig. 6. The OPEA model derived from 149 flares detected in the available short cadence data of KIC 12004834 is shown. In the figure, the filled circles represent the calculated $\log(P)$ values from observations, while the red line represents the OPEA model. The color figure can be viewed online.

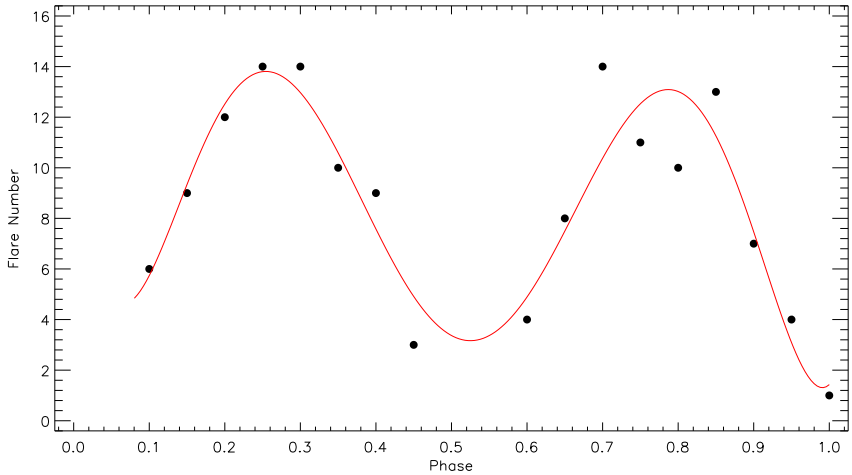


Fig. 7. The distribution of flare total number in each phase interval of 0.05, plotted versus phase for 149 flares. The color figure can be viewed online.

it can be assumed that they are in agreement. In addition, these values indicate that KIC 12004834 is a simple close binary system. Indeed, the possible semi-major axis was found to be as small as $1.84R_{\odot}$ (≈ 0.0086 AU), which indicates that there must be a distance of $0.49R_{\odot}$ between the surfaces of the components. In this case, it is possible that each component can trigger the magnetic activity of the other.

If being in a very close binary affects the chromospheric patterns of the active component, we should see an effect: an increase of the flare frequency or of the *Plateau* value. KIC 12004834 was continuously observed over 89.19 days from JD 24 55739.83568694 to JD 24 55833.27789066, and we detected 149 flare

events. The flare frequency N_1 , the general flare number per an hour, was found to be $0.070 h^{-1}$, while the flare frequency N_2 , the averaged flare energy per an hour, was computed as 0.62 second/hour. However, according to these results, KIC 12004834 did not show a high magnetic activity, not at the expected level.

Comparing the target to similar systems, we can easily notice that like KIC 12004834, both FL Lyr and KIC 9761199 are binary systems, but with high level chromospheric activity. Indeed, the flare frequencies of FL Lyr were recently found to be $N_1 = 0.41632 h^{-1}$ and $N_2 = 0.00027$ by (Yoldaş & Dal 2016). However, the radii of the FL Lyr components were given as $R_1 = 1.283R_{\odot}$, $R_2 = 0.963R_{\odot}$

TABLE 4
THE OPEA MODEL PARAMETERS DERIVED
BY USING THE LEAST-SQUARES METHOD

Parameter	Value
Y_0	-0.197 ± 0.081
<i>Plateau</i>	2.093 ± 0.236
K	0.00048 ± 0.00010
<i>Tau</i>	2098.68
<i>Half-life</i>	1454.7
95% Confidence Intervals	
Y_0	-0.355 to -0.038
<i>Plateau</i>	1.630 to 2.556
K	0.00029 to 0.00067
<i>Tau</i>	1497.65 to 3505.49
<i>Half-life</i>	1038.09 to 2429.82
Goodness of Fit	
R^2	0.7628
<i>p-value</i> (D'Agostino-Pearson)	0.0001
<i>p-value</i> (Shapiro-Wilk)	0.0001
<i>p-value</i> (Kolmogorov-Smirnov)	0.0005

with a semi-major axis of $a = 9.17R_{\odot}$ by Eker et al. (2014). In the case of KIC 9761199, Yoldaş & Dal (2017) found the *Plateau* value as 1.951 s, while the flare frequencies, N_1 and N_2 , were found to be $0.01351 h^{-1}$ and 0.00006 , respectively. The authors computed the masses of the primary and secondary components as $0.57M_{\odot}$, $0.39M_{\odot}$, and the radii of the components as $0.62R_{\odot}$ and $0.56R_{\odot}$ with a semi-major axis of $a = 5.16R_{\odot}$. According to these results, if being a close binary affects the surface magnetic activity, KIC 12004834 should exhibit more frequent or more powerful flares than FL Lyr. On the other hand, according to Dal & Evren (2011); Dal (2012), it is a controversial topic whether the flare frequencies are an indicator of flare activity level, or not. There is one more parameter that may be taken an indicator for the flare activity level, which is the *Plateau* value. The *Plateau* value was found to be 2.093 ± 0.236 s from the OPEA model of KIC 12004834. However, Yoldaş & Dal (2016) found the *Plateau* value as 1.232 ± 0.069 s for FL Lyr. According to these results, the activity level of KIC 12004834 is nearly two times higher than FL Lyr, as expected. With an increasing number of eclipsing binaries with a flaring component, we may determine which parameter is real indicator for the flare activity level.

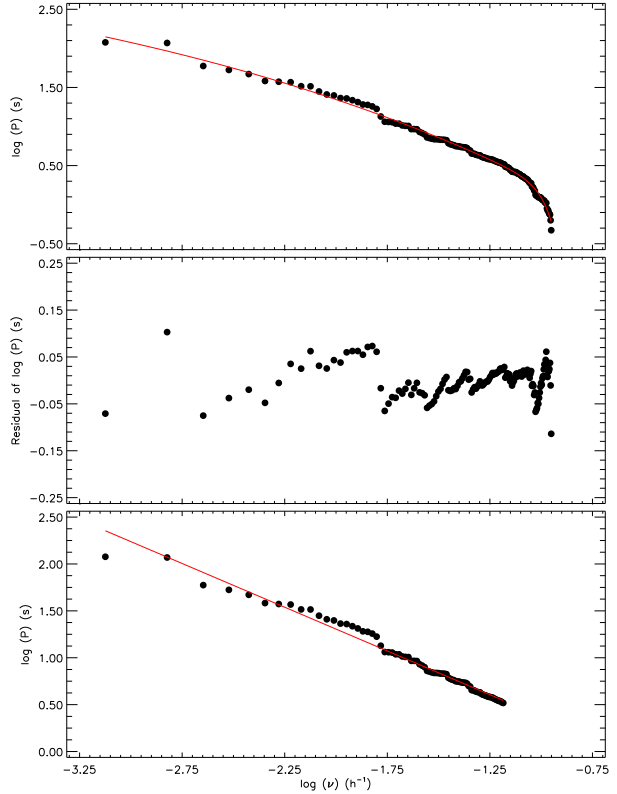


Fig. 8. Cumulative flare frequencies and model computed for 149 flares obtained from KIC 12004834. In the upper panel, the variation of the flare equivalent durations versus the cumulative flare frequency is shown, while the residuals obtained from the model are shown in the middle panel. The bottom panel shows the linear part of the flare energy spectrum and its linear representation. The color figure can be viewed online.

Using the regression calculations, the half-life value was found to be 1454.7 s from the OPEA model for KIC 12004834. In the case of FL Lyr, it is 2291.7 s (Yoldaş & Dal 2016). This means that a flare occurring on FL Lyr can reach the maximum energy level when the flare total duration reaches 38 minutes, while it takes 24.245 minutes for KIC 12004834. Moreover, the maximum flare rise time (T_r) obtained from the flares of KIC 12004834 was found to be 1059.303 s, while the maximum flare total time (T_t) was found to be 5355.050 s. However, these values are $T_r = 5179.00$ s and $T_t = 12770.62$ s for FL Lyr. As a result, the FL Lyr flare time scales are obviously larger than those obtained from KIC 12004834, which is in agreement with the results found by Dal & Evren (2011); Dal (2012) for single flare stars of type dMe.

However, there is one more controversial feature of KIC 12004834, which is stellar spot activity. During the analysis process, we recognised that the synthetic curve derived without any stellar spot does not fit the observations around phase 0.27. Because of this, the results of the light curve analysis point to the presence of stellar spot activity on one of the components. Considering the temperatures of the components we assumed that the flare activity is a sinusoidal variation caused by the rotational modulation due to the stellar cool spots. Indeed, this sinusoidal variation could be easily modelled with a cool spot on the primary component as seen in the 3D model of Roche geometry shown in Figure 4. However, the analyses indicated that the location of the spot is not changed on the primary component along 89.19 day despite the presence of high level flare activity. Considering the rapid variation in the flare behaviour, a stable spotted area on the component is very interesting. According to Hall et al. (1989) and Gershberg (2005), it is well known that the spotted areas on the active components of some RS CVn binaries can keep their shapes and locations for as long as two years. Therefore, the behavior of the cool spot activity observed for KIC 12004834 is not inconsistent with the stellar spot activity phenomenon.

In addition, considering the distribution of the total flare number in each phase interval of 0.05, it is noticed that the flares tend to occur in two specific phases, 0.25 and 0.75, as seen in Figure 7. Since the spotted area is seen around phase 0.27, the behavior of the flare activity of this close binary system KIC 12004834 can be understood.

At this point, one can question whether the sinusoidal variation out-of-eclipses is really caused by the stellar spots. In the literature, Tran et al. (2013) found a way to obtain the sign of the spot activity. They demonstrated that the spot activity remarkably affects the variations of the $(O - C)$ residuals, especially for the $(O - C)_{II}$ residuals. Tran et al. (2013) reported that the stellar spot activity occurring on the active component causes the $(O - C)_{II}$ residuals of both the primary and secondary minima to vary synchronously in a sinusoidal manner, but in opposite directions. We could not determine the minima times from the Kepler long cadence data because the orbital period of KIC 12004834 is short, 0^d.262317. However, we determined all the minima times from the available short cadence data. In the Kepler Mission Database, the short cadence data of observations are covered over 100 days. Because of this, the sinusoidal variation cannot be properly

seen. On the other hand, we determined that the minima times computed from the primary and the secondary minima are separated from each other. This is enough evidence for the spot presence on one component.

We wish to thank the Turkish Scientific and Technical Research Council for supporting this work through grant No. 116F213. We thank the referee for useful comments that have contributed to the improvement of the paper. We also thank Dr. O. Özdarcan for the useful scripts that have supported us, providing an easy way to solve hard calculations.

REFERENCES

- Armstrong, D. J., Gómez Maqueo Chew, Y., Faedi, F., & Pollacco, D. 2014, MNRAS, 437, 3473
 Balona, L. A. 2015, MNRAS, 447, 2714
 Benz, A. O. 2008, LRSP, 5, 1
 Borucki, W. J., Koch, D., Basri, G., et al. 2010, Sci, 327, 977
 Caldwell, D. A., Kolodziejczak, J. J., & Van Cleve, J. E. 2010, ApJL, 713, L92
 Carrington, R. C. 1859, MNRAS, 20, 13
 Coughlin, J. L., López-Morales, M., Harrison, T. E., Ule, N., & Hoffman, D. I. 2011, AJ, 141, 78
 Cutri, R. M., Skrutskie, M. F., van Dyk, S., et al. 2003, The IRSA 2MASS all sky point source catalog. NASA/IPAC Infrared Science Archive <http://irsa.ipac.caltech.edu/applications/Gator>
 D'Agostino, R. B. & Stephens, M. A. 1986, Goodness-Of-Fit Techniques, ed. Ralph B. D'Agostino & M. A. Stephens (New York, NY: Dekker)
 Dal, H. A. 2012, PASJ, 64, 82
 Dal, H. A. & Evren, S. 2010, AJ, 140, 483
 _____ . 2011, AJ, 141, 33
 Dawson, B. & Trapp, R. G. 2004, Basic and Clinical Biostatistics, (New York, NY: McGraw-Hill)
 Debosscher, J., Blomme, J., Aerts, C., & De Ridder, J. 2011, A&A, 529, 89
 Eker, Z., Bilir, S., Soydugan, F., et al. 2014, PASA, 31, 24
 Gershberg, R. E. 2005, Solar-Type Activity in Main-Secauence Stars, (New York, NY: Springer)
 Gershberg, R. E. & Shakhovskaya, N. I. 1983, Ap&SS, 95, 235
 Gershberg, R. E. 1972, Ap&SS, 19, 75
 Green, S. B., Salkind, N. J. & Akey, T. M. 1999, Using SPSS for Windows: Analyzing and Understanding Data (New Jersey, NJ: Perarson)
 Haisch, B., Strong, K. T., & Rodonó, M. 1991, ARA&A, 29, 275
 Hall D. S., Henry G. W., & Sowell J. R. 1989, AJ, 99, 396

- Hodgson, R. 1859, MNRAS, 20, 15
- Ishida, K., Ichimura, K., Shimizu, Y. & Mahasenaputra. 1991, Ap&SS, 182, 227
- Jenkins, J. M., Caldwell, D. A., Chandrasekaran, H., et al. 2010a, ApJL, 713, L87
- Jenkins, J. M., Chandrasekaran, H., McCauliff, S. D., et al. 2010b, SPIE, 7740, 77400
- Kwee, K. K. & van Woerden, H. 1956, BAN, 12, 327
- Koch, D. G., Borucki, W. J., Basri, G., et al. 2010, ApJL, 713, L79
- Lucy, L. B. 1967, ZA, 65, 89
- Matijević, G., Prša, A., Orosz, J. A., et al. 2012, AJ, 143, 123
- Murphy, S. J. 2012, MNRAS, 422, 665
- Murphy, S. J., Shibahashi, H., & Kurtz, D. W. 2013, MNRAS, 430, 2986
- Özdarcan, O., Yoldaş, E., & Dal, H. A. 2018, RMxAA, 54, 37
- Prša, A. & Zwitter, T. 2005, ApJ, 628, 426
- Rodonó, M. 1986, NASSP, 492, 409
- Rucinski, S. M. 1969, AcA, 19, 245
- Slawson, R., Prša, A., Welsh, W. F., et al. 2011, AJ, 142, 160
- Taylor, J. 1997, Introduction to Error Analysis, the Study of Uncertainties in Physical Measurements, (2nd ed.; Sausalito, CA: University Science Books)
- Tokunaga, A. T. 2000, in Allen's Astrophysical Quantities, ed. A. N. Cox (Springer)
- Tran, K., Levine, A., Rappaport, S., et al. 2013, ApJ, 774, 81
- Van Hamme, W. 1993, AJ, 106, 2096
- Walkowicz, L. M. & Basri, G. S. 2013, MNRAS, 436, 1883
- Watson, C. L. 2006, SASS, 25, 47
- Wilson, R. E. 1990, ApJ, 356, 613
- Wilson, R. E. & Devinney, E. J. 1971, ApJ, 166, 605
- Yoldaş, E. & Dal, H. A. 2016, PASA, 33, 16
- _____. 2017, RMxAA, 53, 67